frontiers in MICROBIOLOGY

REVIEW ARTICLE
published: 19 July 2012
doi: 10.3389/fmicb.2012.00258

Molecular dynamics simulation in virus research

Hirotaka Ode[1,2], Masaaki Nakashima[1,3], Shingo Kitamura[1,3], Wataru Sugiura[1,4] and Hironori Sato[2]*

[1] *Clinical Research Center, National Hospital Organization Nagoya Medical Center, Nagoya, Aichi, Japan*
[2] *Pathogen Genomics Center, National Institute of Infectious Diseases, Musashimurayama, Tokyo, Japan*
[3] *Department of Biotechnology, Graduate School of Engineering, Nagoya University, Nagoya, Aichi, Japan*
[4] *Department of AIDS Research, Graduate School of Medicine, Nagoya University, Nagoya, Aichi, Japan*

Edited by:
Masaru Yokoyama, National Institute of Infectious Diseases, Japan

Reviewed by:
Hiroyuki Toh, National Institute of Advanced Industrial Science and Technology, Japan
Yasuyuki Miyazaki, The University of Tokushima Graduate School, Japan

****Correspondence:***
Hirotaka Ode, Department of Infectious Diseases and Immunology, Clinical Research Center, National Hospital Organization Nagoya Medical Center, 4-1-1 Sannomaru, Naka-ku, Nagoya, Aichi, 460-0001, Japan.
e-mail: odehir@nih.go.jp

Virus replication in the host proceeds by chains of interactions between viral and host proteins. The interactions are deeply influenced by host immune molecules and anti-viral compounds, as well as by mutations in viral proteins. To understand how these interactions proceed mechanically and how they are influenced by mutations, one needs to know the structures and dynamics of the proteins. Molecular dynamics (MD) simulation is a powerful computational method for delineating motions of proteins at an atomic-scale via theoretical and empirical principles in physical chemistry. Recent advances in the hardware and software for biomolecular simulation have rapidly improved the precision and performance of this technique. Consequently, MD simulation is quickly extending the range of applications in biology, helping to reveal unique features of protein structures that would be hard to obtain by experimental methods alone. In this review, we summarize the recent advances in MD simulations in the study of virus–host interactions and evolution, and present future perspectives on this technique.

Keywords: MD simulation, viral protein, three-dimensional structure, protein dynamics, coarse-grained MD

INTRODUCTION

Proteins fluctuate spontaneously in solution (Ishima and Torchia, 2000). Accumulating evidence indicates that such fluctuations play key roles in the specific functions of proteins, such as catalytic reactions of enzymes (Nicholson et al., 1995; Lu et al., 1998; Eisenmesser et al., 2005; Henzler-Wildman et al., 2007; Abbondanzieri et al., 2008), interactions with other biomolecules (Thorpe and Brooks, 2007), and biomolecular motors and pumps (Astumian, 1997). Multiple experimental methods are available to characterize the protein dynamics (**Figure 1**). However, it is usually difficult to delineate motions of proteins at an atomic scale.

MD SIMULATION IN BIOLOGY

OUTLINE

Molecular dynamics (MD) simulation is a computational method to address the above issue (**Figure 1**) (Henzler-Wildman and Kern, 2007; Dror et al., 2010). This technique enables us to calculate movements of atoms in a molecular system, such as proteins in water, by numerically solving Newton's equations of motions (Karplus and Petsko, 1990; Adcock and McCammon, 2006). In a simple molecular system, all atoms and covalent bonds connecting the atoms are assumed to be the charged spheres and springs, respectively. Parameters of mathematical functions describing the potential energy of a system, termed the "force field," are set to simulate the movements of atoms and molecules. Frequently used force fields for proteins, such as the "AMBER" (Pearlman et al., 1995; Case et al., 2005) and "CHARMM" (Brooks et al., 2009) force fields, have the formulae of covalent bonds, angles, dihedrals, van der Waals, and electrostatic potentials.

PERFORMANCE AND CONSISTENCY WITH EXPERIMENTAL DATA

Application of MD simulation in the field of protein chemistry was first reported in 1977 (McCammon et al., 1977). Since then, the performance of this technique have been quickly improved quantitatively and qualitatively along with the rapid advances in hardware and software on biomolecular simulation (Lindorff-Larsen et al., 2012). The results of MD simulation are critically influenced by the force fields (Lindorff-Larsen et al., 2012). The qualities of parameters in the force fields, especially for dihedrals and electrostatic potentials, have been improved quantitatively and qualitatively over time by introducing improved approximation to the quantum ground-state potential energy surface. Recently, eight different protein force fields were evaluated on the basis of the consistency of simulations with the NMR data (Lindorff-Larsen et al., 2012). The study demonstrates that the most recent versions, while not perfect, provide results that are highly consistent with the experimental data (Lindorff-Larsen et al., 2012). In addition, explicit introduction of effects of the solvation has contributed to the qualitative improvement for the precision and performance of MD simulations (Adcock and McCammon, 2006).

MD IN STRUCTURAL BIOLOGY

MD simulation currently allows us to investigate the structural dynamics of proteins on timescales of nanoseconds to microseconds, and will probably allow investigation to milliseconds in the future (**Figure 1**) (Henzler-Wildman and Kern, 2007; Dror et al., 2010). This technique is widely used in the field of structural biology (Karplus and McCammon, 2002; Karplus and Kuriyan, 2005; Dodson et al., 2008). First, MD simulation is useful

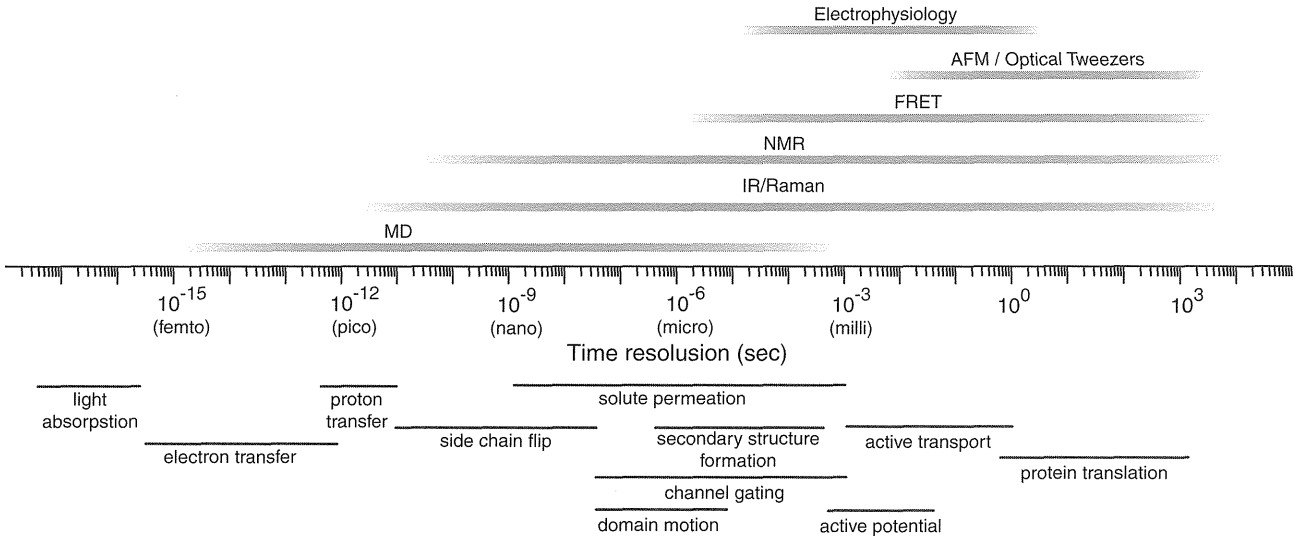

FIGURE 1 | Temporal resolution of various biophysical techniques. The timescales of some fundamental atom- or molecule-scale motions are shown below. AFM, atomic force microscopy; FRET, fluorescence resonance energy transfer; IR, infrared radiation; NMR, nuclear magnetic resonance.

for refining the experimentally determined three-dimensional (3-D) structures of proteins (Autore et al., 2010; Ozen et al., 2011). Second, MD simulation is beneficial for constructing previously undescribed 3-D structures of proteins in combination with homology modeling techniques (Marti-Renom et al., 2000; Sanchez et al., 2000; Baker and Sali, 2001), when a reported structure of a homolog is available. Third and most importantly, MD simulation provides a unique tool to address the structural dynamics of proteins, i.e., the time evolution of conformations in solution, at timescales of nanoseconds to microseconds (Henzler-Wildman and Kern, 2007; Dror et al., 2010). The structural snapshots obtained during MD simulation are helpful for depicting the unique structural features of proteins (Karplus and McCammon, 2002; Karplus and Kuriyan, 2005; Dodson et al., 2008).

MD SIMULATION IN VIROLOGY

To date, MD simulations have been applied in a range of virus researches, as shown in the following sections.

NEUTRALIZATION ESCAPE AND CELL TROPISM SWITCHING OF HIV-1 MEDIATED BY AN ELECTROSTATIC MECHANISM

It is very important to clarify how viruses evade neutralization antibodies in order to understand the viral life cycle and evolution, and to develop vaccines. MD simulation is used to address this issue as it pertains to human immunodeficiency virus type 1 (HIV-1). The third variable (V3) loop of the HIV-1 envelope gp120 protein constitutes the major antibody epitopes of HIV-1 and the major determinants for the entry coreceptor use of HIV-1. By analyzing the 40,000 structural snapshots obtained from 10–30 ns of MD simulations of the identical gp120 outer domain carrying a distinct V3 loop with net charge of +3 or +7, Yokoyama and colleagues showed that the change in V3 net charge alone is sufficient to induce global changes in fluctuation and conformation of the loops involved in binding to CD4, coreceptor, and neutralizing antibodies (Naganawa et al., 2008; Yokoyama et al., 2012). Structural changes caused by a reduction in the V3 net charge via V3 mutations are tightly linked to viral CCR5 coreceptor tropism (Naganawa et al., 2008), as well as to a reduction in viral neutralization sensitivity to anti-V3 antibodies (Naganawa et al., 2008) and anti-CD4 binding site monoclonal antibodies (Yokoyama et al., 2012). These findings suggest a hitherto unrecognized mechanism, V3-mediated electrostatic modulation of the structure and dynamics of the gp120 interaction surface, for adjusting the relative replication fitness and evolution of HIV-1 (Yokoyama et al., 2012). In addition, they partly explain a virological mystery, i.e., why HIV-1 variants using CCR5, which carries a V3 loop with a lower level of positive net charge, predominantly persist before the onset of AIDS.

MECHANISMS OF VIRAL ESCAPE FROM HOST DEFENSE SYSTEMS

Viruses also evade host defense systems other than neutralization antibodies (**Figure 2**). MD simulation is used to clarify the structural basis for viral escape from host defense systems by mutations. Mutations at the 120th amino acid in the HIV-2 capsid protein play a key role in evading tripartite motif-containing protein 5α (TRIM5α), an anti-retroviral cellular protein induced by interferon, both *in vivo* (Onyango et al., 2010) and *in vitro* (Song et al., 2007). An MD simulation study has revealed that the mutations could extensively influence the conformation and fluctuation of the interaction surface of capsid proteins by altering the probability of hydrogen bond formation between helices 4 and 5 (Miyamoto et al., 2011).

HIV-1 Vpu antagonizes an antiviral cellular protein termed tetherin, also known as BST-2/CD317/HM1.24, by interaction with the transmembrane (TM) domain of tetherin and subsequent degradation (Douglas et al., 2010; Kobayashi et al., 2011). An MD simulation suggests that alignment of the four

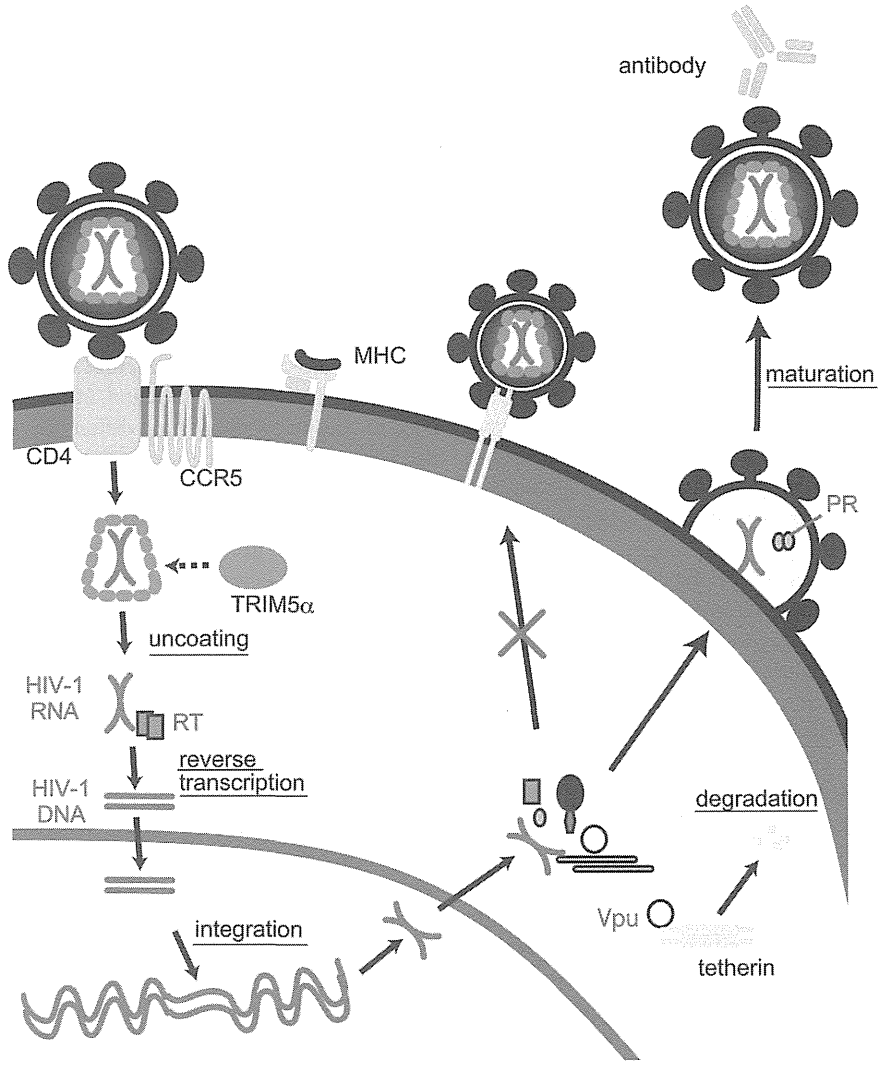

FIGURE 2 | Life cycle of HIV-1 and interactions between viral proteins and host immune molecules.

amino acid residues (I34, L37, L41, and T45) on the same helical face in the human tetherin TM domain is crucial for the Vpu-mediated antagonism against human tetherin (Kobayashi et al., 2011). The interface structure of the tetherin TM for the antagonism was also predicted by the MD simulation of another group (Zhou et al., 2012) and experimentally confirmed by an NMR study (Skasko et al., 2012).

MD simulation is also used to study the mechanisms of functional interactions between cytotoxic T lymphocyte (CTL) epitope and major histocompatibility complex (MHC) molecules (Reboul et al., 2012). An MD simulation study has revealed that a 13-mer epitope peptide from Epstein-Barr virus has the low structural flexibility in an MHC molecule that induces a CTL response but exhibits high flexibility in another MHC molecule that cannot induce a CTL response (Reboul et al., 2012). Thus, structural flexibility of CTL epitope region seems to be critical for the specific recognition by MHC molecules, and mutations that alter the flexibility may influence CTL response. There are other viral proteins and immune molecules involved in viral evasion from host defense systems (Neil and Bieniasz, 2009; Malim and Bieniasz, 2012). MD simulations should also be applicable for the studies of these molecules.

STRUCTURE AND FUNCTION OF VIRAL ENZYMES

Viral enzymes are essential for viral replications and thus are important targets for anti-viral drug development. MD simulations are used to study the basis of the structural dynamics that allow the viral enzyme and its drug to function properly. Viral polymerase (Pol) is essential for viral genome replication in the viral life cycle. The Pol is composed of the fingers, palm, and thumb subdomains, which form a cavity for the substrate binding, as in eukaryotic Pol (Joyce and Steitz, 1994; Lamers et al., 2006; Cameron et al., 2009). MD simulations suggest that the finger and thumb domains of HIV-1 reverse transcriptase (RT) are especially mobile among the various regions of this enzyme (Zhou et al., 2005; Kirmizialtin et al., 2012). The mobility

is severely attenuated by binding of allosteric non-nucleotide RT inhibitors (NNRTIs) (Zhou et al., 2005). Interestingly, a large conformational change of RT subdomains during millisecond timescale simulations can lock the correct nucleotide at the active site but promotes release of a mismatched nucleotide (Kirmizialtin et al., 2012). Furthermore, conformational dynamics leading to opening and closing motions of the substrate binding cleft are highly conserved among four RNA Pols in the picornavirus family, despite the amino acid identity being as low as 30–74% (Moustafa et al., 2011). These findings are consistent with each other and strongly suggest that the structural dynamics of viral Pol play a key role in the polymerization.

Viral protease (PR) plays a key role in viral propagation by catalyzing cleavages of viral precursor proteins (Pettit et al., 1994, 2002; Steven et al., 2005). HIV-1 PR and other retroviral PRs have unique regions termed the "flaps" outside the substrate binding clefts (Dunn et al., 2002). MD simulation studies suggest that the PR flaps in HIV-1 are intrinsically mobile, undergoing conversions between the "semiopen," "open," and "closed" conformations (Hornak et al., 2006; Deng et al., 2011). This movement is severely attenuated upon placement of the substrate or PR inhibitor in the binding cleft (Karthik and Senapati, 2011), suggesting that flap movement plays a critical role in PR function.

MD simulations are also used to study the structural dynamics of the substrates of viral PR. Peptides corresponding to cleavage junctions of viral precursor proteins of HIV-1 are intrinsically unstructured in aqueous solution (Datta et al., 2011; Ode et al., 2011). However, the folding preference of the junction peptides may be different among the junctions and related to the efficiency of substrate binding and cleavage reaction by PR (Ode et al., 2011). Furthermore, peptides at the capsid-p2 junction can adopt a helical conformation when the polarity of the environment is reduced (Datta et al., 2011). The MD simulation of PR and its substrates will help to clarify how the viral precursor is processed orderly during viral maturation.

DRUG-RESISTANCE MECHANISMS

Antiviral drug resistance is a major clinical problem for the treatment of virus-infected individuals (Cortez and Maldarelli, 2011; van der Vries et al., 2011). Viral resistance to antiviral drugs is primarily caused by genetic mutations that eventually lead to a reduction in the drug affinity of drug target viral proteins. MD simulations are used to examine how viral mutations cause the drug resistance at the atomic level.

A reduction in the binding affinity of the PR inhibitors to HIV-1 PR can be caused by a reduction in hydrophobic interactions (Kagan et al., 2005; Wittayanarakul et al., 2005; Sadiq et al., 2007; Chen et al., 2010; Dirauf et al., 2010), reduction in electrostatic interactions (Ode et al., 2005, 2006, 2007a; Chen et al., 2010), changes in flexibility at the flap of the PR (Piana et al., 2002; Perryman et al., 2004; Chang et al., 2006; Foulkes-Murzycki et al., 2007), and changes in the shape of the inhibitor-binding pocket (Ode et al., 2005, 2006, 2007b). Reduction in binding affinity of the nucleotide/nucleoside RT inhibitors (NRTIs) to HIV-1 RT can be caused by a distinct conformational preference of NRTIs in the substrate/NRTI-binding site compared to normal substrates (Carvalho et al., 2006) or enhancement of ATP-mediated excision of misincorporated nucleotide analogs via increased accessibility of ATP to the terminus of extending DNA (White et al., 2004; Carvalho et al., 2007). Reduction in the binding affinity of the NNRTIs to HIV-1 RT can be attained by occlusion of the NNRTI-entry pathway (Rodriguez-Barrios and Gago, 2004; Rodriguez-Barrios et al., 2005) or restoration of the proper flexibility of the RT even with NNRTIs (Zhou et al., 2005).

A change in volume of the binding site of influenza virus (IFV) M2 channel blockers has been shown to reduce the blockers' binding affinity (Gu et al., 2011; Leonov et al., 2011; Wang et al., 2011). Disruption of the proper guidance of IFV neuraminidase (NA) inhibitors into their binding pocket is proposed as a possible mechanism for the reduction in the binding affinity of the inhibitors (Le et al., 2010; Kasson, 2012). MD simulations are also used to study how the genetic differences of HIV variants around the world can influence the efficacy of antiviral inhibitors (Batista et al., 2006; Ode et al., 2007a; Matsuyama et al., 2010; Soares et al., 2010; Kar and Knecht, 2012). Thus, MD simulation will be valuable to assist in the study of drug efficacy when genetic information on the drug target proteins is available (Shenderovich et al., 2003; Stoica et al., 2008; Sadiq et al., 2010; Wright and Coveney, 2011).

ANTIVIRAL DRUG DISCOVERY AND DEVELOPMENT

MD simulations are used to assist in the discovery and development of antiviral drugs (Durrant and McCammon, 2011; Borhani and Shaw, 2012). MD simulations allow sampling snapshots of fluctuated protein structures, which include their short-lived conformations as well as stable conformations. This is beneficial for searching conformations of a protein on ligand-binding, since ligand-binding can stabilize conformation of a protein that is not the most stable at ligand-free state (Tobi and Bahar, 2005; Xu et al., 2008). Thus, the MD simulations are used to improve the enrichment performance of molecular docking during *in silico* drug screening by taking accounts of multiple docking poses (Okimoto et al., 2009). The method is also applied for identifying concealed drug-binding sites, which are apparently masked and not evident from the X-ray crystal structures, by considering the structural flexibility of proteins. For example, MD simulations have been used to find a trench adjacent to the active site of HIV-1 integrase (Schames et al., 2004). A site-directed mutagenesis study provided evidence that the trench indeed plays key roles in ligand-binding (Lee and Robinson, 2006). These findings have been used to design HIV-1 integrase inhibitors with potent antiviral effects (Durrant and McCammon, 2011).

Likewise, MD simulations are used to assist in the development of antiviral drugs against IFV. Using this method, a universal cavity adjacent to the binding site of natural substrate has been reported with NA proteins of human 2009 pandemic H1N1, avian H5N1, and human H2N2 strains (Amaro et al., 2011). MD simulations were also used to construct a 3-D structure model of CCR5, a major coreceptor of HIV-1 (Maeda et al., 2008; Da and Wu, 2011).

VIRION STRUCTURE

It is essential to clarify the structure of virions in order to understand the mechanisms of viral infection and assembly.

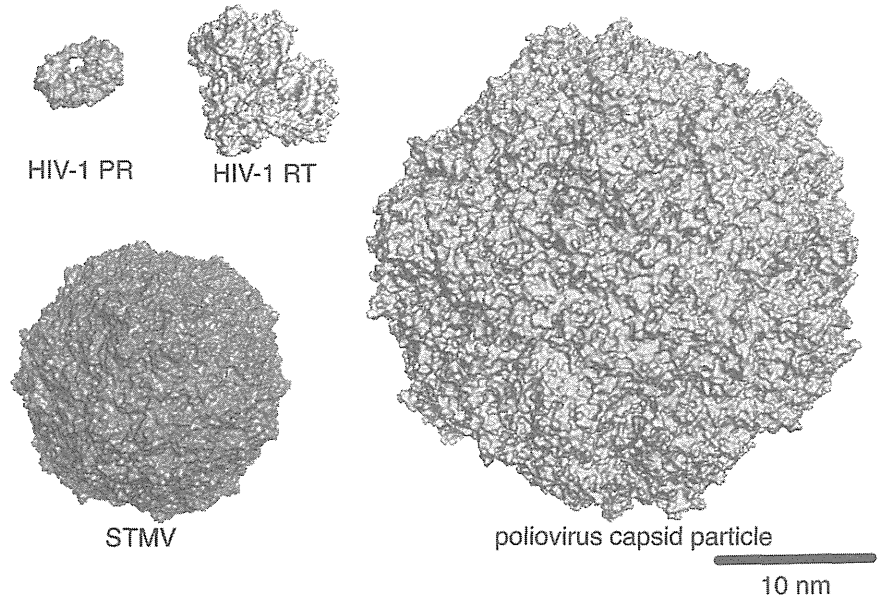

FIGURE 3 | Molecular scales of viral proteins and capsid particles. The structures of HIV-1 PR (PDB code: 1HHP), HIV-1 RT (PDB code: 1RTD), STMV (PDB code: 1A34), and poliovirus capsid particle (PDB code: 1HXS), which are deposited in the Protein Data Bank (PDB) (http://www.rcsb.org/pdb/home/home.do) or the VIPERdb (http://viperdb.scripps.edu/), are shown in surface representation.

MD simulation is used to address this issue. Using a super computer, Freddolino et al. performed 50-nanosecond-timescale MD simulations of the symmetric structure of a complete satellite tobacco mosaic virus (STMV) particle containing about 1 million atoms (Arkhipov et al., 2006) (**Figure 3**). Thus, far, this is one of the largest systems among the MD simulations reported in all biological fields. Notably, the virion with viral RNA was stable during the simulations, whereas the one without the RNA was unstable, suggesting that viral RNA plays a key role in stabilizing the STMV virion (Arkhipov et al., 2006). The study is consistent with the experimental data (Day et al., 2001) and therefore provides a set of rationale conditions for performing the MD simulation of virion. Likewise, Larsson et al. reported about 1-microsecond-timescale MD simulations of the satellite tobacco necrosis virus (STNV) (Larsson et al., 2012). Their study reproduced the biochemical phenomenon of the STNV virion in solution (Unge et al., 1986), i.e., the swelling of capsid upon Ca^{2+} removal by EDTA treatment. These findings will provide a structural basis for identifying the key regulators of assembly and infections and for illustrating how they function mechanically. Although MD simulation of virions composed of very large numbers of atoms is still difficult in most cases, progress in the hardware and software for the simulation, together with the accumulation of biological and physicochemical information on virions, will help us to overcome these limitations in the MD simulation of virions.

PERSPECTIVE

Since the processing speed of computers is still doubling approximately every two years according to Moore's law, MD studies will be extended to simulations of larger and more complex system at longer timescales. This will then lead to a better understanding of the structures and dynamics of macromolecules involved in virus–host interactions.

COARSE-GRAINED (CG) MD SIMULATIONS

MD simulations of macromolecules consisting of large molecular systems, such as oligomeric proteins, macromolecular complexes, and membrane proteins in a lipid bilayer, and virions are desired to better understand viruses. However, such simulations require unrealistically long analytical times and high-performance computers at present, and thereby are still limited mostly to the small molecules (Henzler-Wildman and Kern, 2007; Dror et al., 2010). To cope with this issue and to improve the practicability of long timescale MD simulation, a "coarse-grained (CG) MD" simulation has been developed (Merchant and Madura, 2011; Takada, 2012). The CG-MD simulation employs "pseudo-atoms" that consist of several atoms in a group and calculates the movement of these "pseudo-atoms" rather than the movement of "individual atoms," thereby greatly reducing the calculation time (Merchant and Madura, 2011; Takada, 2012). CG-MD simulations have been used to study helicases of hepatitis C virus (HCV) and simian virus 40 and have successfully reproduced enzyme motions, such as "ratcheting inchworm translocation" and "spring-loaded DNA unwinding" (Flechsig and Mikhailov, 2010; Yoshimoto et al., 2010). Briefly, the ratcheting inchworm translocation is the unidirectional motion of the HCV NS3 helicase during translocation that occurs by the step size of one base per ATP hydrolysis cycle (Gu and Rice, 2010). Meanwhile, the spring-loaded DNA unwinding is the discrete steps of unwinding of DNA by the HCV NS3 helicase that occurs periodically via a burst of 3-bp unwinding during NS3 translocation consuming ATPs (Myong et al., 2007).

CG-MD has also been applied to the study of the structural characteristics and stabilities of the capsid particle and virion (**Figure 3**). Such studies have been used to investigate small plant viruses (~28 nanometer in diameter), such as the three satellite plant viruses STMV, STNV, and the satellite panicum mosaic virus (SPMV), as well as the brome mosaic virus (BMV) (Arkhipov et al., 2006, 2009), and more complex capsids such as poliovirus (Arkhipov et al., 2006, 2009), asymmetric, conical-shaped HIV-1 capsid particles (Krishna et al., 2010), and the immature HIV-1 virion (Ayton and Voth, 2010). These studies have predicted various molecular interactions that can be tested experimentally. Thus, CG-MD may play a pivotal role in the MD study of micrometer-sized systems at millisecond timescale (Merchant and Madura, 2011; Takada, 2012) and therefore may uncover novel characteristics of the interactions in virus–host relationships.

INTRINSICALLY DISORDERED PROTEINS

Some eukaryotic proteins have no stable 3-D structure under physiological conditions (Dunker et al., 2002, 2008; Dyson and Wright, 2005). These proteins are referred to as intrinsically disordered, natively unfolded, or intrinsically unstructured proteins. They undergo structural transition from a disordered to an ordered state upon binding to target molecules such as proteins, DNA, and small molecules (Dunker et al., 2005; Sandhu and Dash, 2007). They are often related to the "hub proteins" that have many binding partners and control important biological processes (Iakoucheva et al., 2002; Haynes et al., 2006; Sandhu, 2009). Interestingly, viral proteins or portions of viral proteins are often intrinsically disordered. These include genome-linked protein VPg protein of plant viruses (Grzela et al., 2008; Rantalainen et al., 2008; Jiang and Laliberte, 2011; Rantalainen et al., 2011), HIV-1 Tat (Shojania and O'Neil, 2010), and Vif proteins (Reingewertz et al., 2010), and paramyxovirus nucleoproteins and phosphoproteins (Habchi and Longhi, 2012). It has been proposed that the disordered structure is beneficial for viruses to gain multiple functions in the viral life cycle with limited genome size (Rantalainen et al., 2011; Habchi and Longhi, 2012; Xue et al., 2012). Clarifying the folding landscape of viral proteins by standard MD and CG-MD simulations may help in understanding the structural principles by which viral proteins execute multiple functions in the viral life cycle.

ACKNOWLEDGMENTS

The MD studies of our laboratory described in this article are supported by grants from the Ministry of Health, Labor and Welfare for HIV/AIDS research and by a Grant-in-Aid for JSPS Fellows.

REFERENCES

Abbondanzieri, E. A., Bokinsky, G., Rausch, J. W., Zhang, J. X., Le Grice, S. F., and Zhuang, X. (2008). Dynamic binding orientations direct activity of HIV reverse transcriptase. *Nature* 453, 184–189.

Adcock, S. A., and McCammon, J. A. (2006). Molecular dynamics: survey of methods for simulating the activity of proteins. *Chem. Rev.* 106, 1589–1615.

Amaro, R. E., Swift, R. V., Votapka, L., Li, W. W., Walker, R. C., and Bush, R. M. (2011). Mechanism of 150-cavity formation in influenza neuraminidase. *Nat. Commun.* 2, 388.

Arkhipov, A., Freddolino, P. L., and Schulten, K. (2006). Stability and dynamics of virus capsids described by coarse-grained modeling. *Structure* 14, 1767–1777.

Arkhipov, A., Roos, W. H., Wuite, G. J., and Schulten, K. (2009). Elucidating the mechanism behind irreversible deformation of viral capsids. *Biophys. J.* 97, 2061–2069.

Astumian, R. D. (1997). Thermodynamics and kinetics of a brownian motor. *Science* 276, 917–922.

Autore, F., Bergeron, J. R., Malim, M. H., Fraternali, F., and Huthoff, H. (2010). Rationalisation of the differences between APOBEC3G structures from crystallography and NMR studies by molecular dynamics simulations. *PLoS ONE* 5:e11515. doi: 10.1371/journal.pone.0011515

Ayton, G. S., and Voth, G. A. (2010). Multiscale computer simulation of the immature HIV-1 virion. *Biophys. J.* 99, 2757–2765.

Baker, D., and Sali, A. (2001). Protein structure prediction and structural genomics. *Science* 294, 93–96.

Batista, P. R., Wilter, A., Durham, E. H., and Pascutti, P. G. (2006). Molecular dynamics simulations applied to the study of subtypes of HIV-1 protease common to Brazil, Africa, and Asia. *Cell Biochem. Biophys.* 44, 395–404.

Borhani, D. W., and Shaw, D. E. (2012). The future of molecular dynamics simulations in drug discovery. *J. Comput. Aided. Mol. Des.* 26, 15–26.

Brooks, B. R., Brooks, C. L. 3rd., Mackerell, A. D. Jr., Nilsson, L., Petrella, R. J., Roux, B., Won, Y., Archontis, G., Bartels, C., Boresch, S., Caflisch, A., Caves, L., Cui, Q., Dinner, A. R., Feig, M., Fischer, S., Gao, J., Hodoscek, M., Im, W., Kuczera, K., Lazaridis, T., Ma, J., Ovchinnikov, V., Paci, E., Pastor, R. W., Post, C. B., Pu, J. Z., Schaefer, M., Tidor, B., Venable, R. M., Woodcock, H. L., Wu, X., Yang, W., York, D. M., and Karplus, M. (2009). CHARMM: the biomolecular simulation program. *J. Comput. Chem.* 30, 1545–1614.

Cameron, C. E., Moustafa, I. M., and Arnold, J. J. (2009). Dynamics: the missing link between structure and function of the viral RNA-dependent RNA polymerase? *Curr. Opin. Struct. Biol.* 19, 768–774.

Carvalho, A. T., Fernandes, P. A., and Ramos, M. J. (2006). Insights on resistance to reverse transcriptase: the different patterns of interaction of the nucleoside reverse transcriptase inhibitors in the deoxyribonucleotide triphosphate binding site relative to the normal substrate. *J. Med. Chem.* 49, 7675–7682.

Carvalho, A. T., Fernandes, P. A., and Ramos, M. J. (2007). The excision mechanism in reverse transcriptase: pyrophosphate leaving and fingers opening are uncoupled events with the analogues AZT and d4T. *J. Phys. Chem. B* 111, 12032–12039.

Case, D. A., Cheatham, T. E., 3rd, Darden, T., Gohlke, H., Luo, R., Merz, K. M. Jr., Onufriev, A., Simmerling, C., Wang, B., and Woods, R. J. (2005). The amber biomolecular simulation programs. *J. Comput. Chem.* 26, 1668–1688.

Chang, C. E., Shen, T., Trylska, J., Tozzini, V., and McCammon, J. A. (2006). Gated binding of ligands to HIV-1 protease: brownian dynamics simulations in a coarse-grained model. *Biophys. J.* 90, 3880–3885.

Chen, J., Zhang, S., Liu, X., and Zhang, Q. (2010). Insights into drug resistance of mutations D30N and I50V to HIV-1 protease inhibitor TMC-114, free energy calculation and molecular dynamic simulation. *J. Mol. Model.* 16, 459–468.

Cortez, K. J., and Maldarelli, F. (2011). Clinical management of HIV drug resistance. *Viruses* 3, 347–378.

Da, L. T., and Wu, Y. D. (2011). Theoretical studies on the interactions and interferences of HIV-1 glycoprotein gp120 and its coreceptor CCR5. *J. Chem. Inf. Model.* 51, 359–369.

Datta, S. A., Temeselew, L. G., Crist, R. M., Soheilian, F., Kamata, A., Mirro, J., Harvin, D., Nagashima, K., Cachau, R. E., and Rein, A. (2011). On the role of the SP1 domain in HIV-1 particle assembly: a molecular switch? *J. Virol.* 85, 4111–4121.

Day, J., Kuznetsov, Y. G., Larson, S. B., Greenwood, A., and McPherson, A. (2001). Biophysical studies on the RNA cores of satellite tobacco mosaic virus. *Biophys. J.* 80, 2364–2371.

Deng, N. J., Zheng, W., Gallicchio, E., and Levy, R. M. (2011). Insights into the dynamics of HIV-1 protease: a kinetic network

model constructed from atomistic simulations. *J. Am. Chem. Soc.* 133, 9387–9394.

Dirauf, P., Meiselbach, H., and Sticht, H. (2010). Effects of the V82A and I54V mutations on the dynamics and ligand binding properties of HIV-1 protease. *J. Mol. Model.* 16, 1577–1583.

Dodson, G. G., Lane, D. P., and Verma, C. S. (2008). Molecular simulations of protein dynamics: new windows on mechanisms in biology. *EMBO Rep.* 9, 144–150.

Douglas, J. L., Gustin, J. K., Viswanathan, K., Mansouri, M., Moses, A. V., and Fruh, K. (2010). The great escape: viral strategies to counter BST-2/tetherin. *PLoS Pathog.* 6:e1000913. doi: 10.1371/journal.ppat.1000913

Dror, R. O., Jensen, M. O., Borhani, D. W., and Shaw, D. E. (2010). Exploring atomic resolution physiology on a femtosecond to millisecond timescale using molecular dynamics simulations. *J. Gen. Physiol.* 135, 555–562.

Dunker, A. K., Brown, C. J., Lawson, J. D., Iakoucheva, L. M., and Obradovic, Z. (2002). Intrinsic disorder and protein function. *Biochemistry* 41, 6573–6582.

Dunker, A. K., Cortese, M. S., Romero, P., Iakoucheva, L. M., and Uversky, V. N. (2005). Flexible nets. The roles of intrinsic disorder in protein interaction networks. *FEBS J.* 272, 5129–5148.

Dunker, A. K., Silman, I., Uversky, V. N., and Sussman, J. L. (2008). Function and structure of inherently disordered proteins. *Curr. Opin. Struct. Biol.* 18, 756–764.

Dunn, B. M., Goodenow, M. M., Gustchina, A., and Wlodawer, A. (2002). Retroviral proteases. *Genome Biol.* 3, Reviews3006.

Durrant, J. D., and McCammon, J. A. (2011). Molecular dynamics simulations and drug discovery. *BMC Biol.* 9, 71.

Dyson, H. J., and Wright, P. E. (2005). Intrinsically unstructured proteins and their functions. *Nat. Rev. Mol. Cell. Biol.* 6, 197–208.

Eisenmesser, E. Z., Millet, O., Labeikovsky, W., Korzhnev, D. M., Wolf-Watz, M., Bosco, D. A., Skalicky, J. J., Kay, L. E., and Kern, D. (2005). Intrinsic dynamics of an enzyme underlies catalysis. *Nature* 438, 117–121.

Flechsig, H., and Mikhailov, A. S. (2010). Tracing entire operation cycles of molecular motor hepatitis C virus helicase in structurally resolved dynamical simulations. *Proc. Natl. Acad. Sci. U.S.A.* 107, 20875–20880.

Foulkes-Murzycki, J. E., Scott, W. R., and Schiffer, C. A. (2007). Hydrophobic sliding: a possible mechanism for drug resistance in human immunodeficiency virus type 1 protease. *Structure* 15, 225–233.

Grzela, R., Szolajska, E., Ebel, C., Madern, D., Favier, A., Wojtal, I., Zagorski, W., and Chroboczek, J. (2008). Virulence factor of potato virus Y, genome-attached terminal protein VPg, is a highly disordered protein. *J. Biol. Chem.* 283, 213–221.

Gu, M., and Rice, C. M. (2010). Three conformational snapshots of the hepatitis C virus NS3 helicase reveal a ratchet translocation mechanism. *Proc. Natl. Acad. Sci. U.S.A.* 107, 521–528.

Gu, R. X., Liu, L. A., Wei, D. Q., Du, J. G., Liu, L., and Liu, H. (2011). Free energy calculations on the two drug binding sites in the M2 proton channel. *J. Am. Chem. Soc.* 133, 10817–10825.

Habchi, J., and Longhi, S. (2012). Structural disorder within paramyxovirus nucleoproteins and phosphoproteins. *Mol. Biosyst.* 8, 69–81.

Haynes, C., Oldfield, C. J., Ji, F., Klitgord, N., Cusick, M. E., Radivojac, P., Uversky, V. N., Vidal, M., and Iakoucheva, L. M. (2006). Intrinsic disorder is a common feature of hub proteins from four eukaryotic interactomes. *PLoS Comput. Biol.* 2:e100. doi: 10.1371/journal.pcbi.0020100

Henzler-Wildman, K., and Kern, D. (2007). Dynamic personalities of proteins. *Nature* 450, 964–972.

Henzler-Wildman, K. A., Lei, M., Thai, V., Kerns, S. J., Karplus, M., and Kern, D. (2007). A hierarchy of timescales in protein dynamics is linked to enzyme catalysis. *Nature* 450, 913–916.

Hornak, V., Okur, A., Rizzo, R. C., and Simmerling, C. (2006). HIV-1 protease flaps spontaneously open and reclose in molecular dynamics simulations. *Proc. Natl. Acad. Sci. U.S.A.* 103, 915–920.

Iakoucheva, L. M., Brown, C. J., Lawson, J. D., Obradovic, Z., and Dunker, A. K. (2002). Intrinsic disorder in cell-signaling and cancer-associated proteins. *J. Mol. Biol.* 323, 573–584.

Ishima, R., and Torchia, D. A. (2000). Protein dynamics from NMR. *Nat. Struct. Biol.* 7, 740–743.

Jiang, J., and Laliberte, J. F. (2011). The genome-linked protein VPg of plant viruses-a protein with many partners. *Curr. Opin. Virol.* 1, 347–354.

Joyce, C. M., and Steitz, T. A. (1994). Function and structure relationships in DNA polymerases. *Annu. Rev. Biochem.* 63, 777–822.

Kagan, R. M., Shenderovich, M. D., Heseltine, P. N., and Ramnarayan, K. (2005). Structural analysis of an HIV-1 protease I47A mutant resistant to the protease inhibitor lopinavir. *Protein Sci.* 14, 1870–1878.

Kar, P., and Knecht, V. (2012). Origin of decrease in potency of darunavir and two related antiviral inhibitors against HIV-2 compared to HIV-1 protease. *J. Phys. Chem. B* 116, 2605–2614.

Karplus, M., and Kuriyan, J. (2005). Molecular dynamics and protein function. *Proc. Natl. Acad. Sci. U.S.A.* 102, 6679–6685.

Karplus, M., and McCammon, J. A. (2002). Molecular dynamics simulations of biomolecules. *Nat. Struct. Biol.* 9, 646–652.

Karplus, M., and Petsko, G. A. (1990). Molecular dynamics simulations in biology. *Nature* 347, 631–639.

Karthik, S., and Senapati, S. (2011). Dynamic flaps in HIV-1 protease adopt unique ordering at different stages in the catalytic cycle. *Proteins* 79, 1830–1840.

Kasson, P. M. (2012). Receptor binding by influenza virus: using computational techniques to extend structural data. *Biochemistry* 51, 2359–2365.

Kirmizialtin, S., Nguyen, V., Johnson, K. A., and Elber, R. (2012). How conformational dynamics of DNA polymerase select correct substrates: experiments and simulations. *Structure* 20, 618–627.

Kobayashi, T., Ode, H., Yoshida, T., Sato, K., Gee, P., Yamamoto, S. P., Ebina, H., Strebel, K., Sato, H., and Koyanagi, Y. (2011). Identification of amino acids in the human tetherin transmembrane domain responsible for HIV-1 Vpu interaction and susceptibility. *J. Virol.* 85, 932–945.

Krishna, V., Ayton, G. S., and Voth, G. A. (2010). Role of protein interactions in defining HIV-1 viral capsid shape and stability: a coarse-grained analysis. *Biophys. J.* 98, 18–26.

Lamers, M. H., Georgescu, R. E., Lee, S. G., O'Donnell, M., and Kuriyan, J. (2006). Crystal structure of the catalytic alpha subunit of E. coli replicative DNA polymerase III. *Cell* 126, 881–892.

Larsson, D. S., Liljas, L., and van der Spoel, D. (2012). Virus capsid dissolution studied by microsecond molecular dynamics simulations. *PLoS Comput. Biol.* 8:e1002502. doi: 10.1371/journal.pcbi.1002502

Le, L., Lee, E. H., Hardy, D. J., Truong, T. N., and Schulten, K. (2010). Molecular dynamics simulations suggest that electrostatic funnel directs binding of Tamiflu to influenza N1 neuraminidases. *PLoS Comput. Biol.* 6:e1000939. doi: 10.1371/journal.pcbi.1000939

Lee, D. J., and Robinson, W. E. Jr. (2006). Preliminary mapping of a putative inhibitor-binding pocket for human immunodeficiency virus type 1 integrase inhibitors. *Antimicrob. Agents Chemother.* 50, 134–142.

Leonov, H., Astrahan, P., Krugliak, M., and Arkin, I. T. (2011). How do aminoadamantanes block the influenza M2 channel, and how does resistance develop? *J. Am. Chem. Soc.* 133, 9903–9911.

Lindorff-Larsen, K., Maragakis, P., Piana, S., Eastwood, M. P., Dror, R. O., and Shaw, D. E. (2012). Systematic validation of protein force fields against experimental data. *PLoS ONE* 7:e32131. doi: 10.1371/journal.pone.0032131

Lu, H. P., Xun, L., and Xie, X. S. (1998). Single-molecule enzymatic dynamics. *Science* 282, 1877–1882.

Maeda, K., Das, D., Yin, P. D., Tsuchiya, K., Ogata-Aoki, H., Nakata, H., Norman, R. B., Hackney, L. A., Takaoka, Y., and Mitsuya, H. (2008). Involvement of the second extracellular loop and transmembrane residues of CCR5 in inhibitor binding and HIV-1 fusion: insights into the mechanism of allosteric inhibition. *J. Mol. Biol.* 381, 956–974.

Malim, M. H., and Bieniasz, P. D. (2012). HIV restriction factors and mechanisms of evasion. *Cold Spring Harb. Perspect. Med.* 2, a006940.

Marti-Renom, M. A., Stuart, A. C., Fiser, A., Sanchez, R., Melo, F., and Sali, A. (2000). Comparative protein structure modeling of genes and genomes. *Annu. Rev. Biophys. Biomol. Struct.* 29, 291–325.

Matsuyama, S., Aydan, A., Ode, H., Hata, M., Sugiura, W., and Hoshino, T. (2010). Structural and energetic analysis on the complexes of clinically isolated subtype C HIV-1 proteases and approved inhibitors by molecular dynamics simulation. *J. Phys. Chem. B* 114, 521–530.

McCammon, J. A., Gelin, B. R., and Karplus, M. (1977). Dynamics of folded proteins. *Nature* 267, 585–590.

Merchant, B. A., and Madura, J. D. (2011). A review of coarse-grained molecular dynamics techniques to access extended spatial and temporal scales in biomolecular simulations. *Annu. Rep. Comput. Chem.* 7, 67–87.

Miyamoto, T., Yokoyama, M., Kono, K., Shioda, T., Sato, H., and Nakayama, E. E. (2011). A single amino acid of human immunodeficiency virus type 2 capsid protein affects conformation of two external loops and viral sensitivity to TRIM5alpha. *PLoS ONE* 6:e22779. doi: 10.1371/journal.pone.0022779

Moustafa, I. M., Shen, H., Morton, B., Colina, C. M., and Cameron, C. E. (2011). Molecular dynamics simulations of viral RNA polymerases link conserved and correlated motions of functional elements to fidelity. *J. Mol. Biol.* 410, 159–181.

Myong, S., Bruno, M. M., Pyle, A. M., and Ha, T. (2007). Spring-loaded mechanism of DNA unwinding by hepatitis C virus NS3 helicase. *Science* 317, 513–516.

Naganawa, S., Yokoyama, M., Shiino, T., Suzuki, T., Ishigatsubo, Y., Ueda, A., Shirai, A., Takeno, M., Hayakawa, S., Sato, S., Tochikubo, O., Kiyoura, S., Sawada, K., Ikegami, T., Kanda, T., Kitamura, K., and Sato, H. (2008). Net positive charge of HIV-1 CRF01_AE V3 sequence regulates viral sensitivity to humoral immunity. *PLoS ONE* 3:e3206. doi: 10.1371/journal.pone.0003206

Neil, S., and Bieniasz, P. (2009). Human immunodeficiency virus, restriction factors, and interferon. *J. Interferon Cytokine Res.* 29, 569–580.

Nicholson, L. K., Yamazaki, T., Torchia, D. A., Grzesiek, S., Bax, A., Stahl, S. J., Kaufman, J. D., Wingfield, P. T., Lam, P. Y. S., Jadhav, P. K., Hodge, C. N., Domaille, P. J., and Chang, C.-H. (1995). Flexibility and function in HIV-1 protease. *Nat. Struct. Biol.* 2, 274–280.

Ode, H., Matsuyama, S., Hata, M., Hoshino, T., Kakizawa, J., and Sugiura, W. (2007a). Mechanism of drug resistance due to N88S in CRF01_AE HIV-1 protease, analyzed by molecular dynamics simulations. *J. Med. Chem.* 50, 1768–1777.

Ode, H., Matsuyama, S., Hata, M., Neya, S., Kakizawa, J., Sugiura, W., and Hoshino, T. (2007b). Computational characterization of structural role of the non-active site mutation M36I of human immunodeficiency virus type 1 protease. *J. Mol. Biol.* 370, 598–607.

Ode, H., Neya, S., Hata, M., Sugiura, W., and Hoshino, T. (2006). Computational simulations of HIV-1 proteases - multi-drug resistance due to nonactive site mutation L90M. *J. Am. Chem. Soc.* 128, 7887–7895.

Ode, H., Ota, M., Neya, S., Hata, M., Sugiura, W., and Hoshino, T. (2005). Resistant mechanism against nelfinavir of human immunodeficiency virus type 1 proteases. *J. Phys. Chem. B* 109, 565–574.

Ode, H., Yokoyama, M., Kanda, T., and Sato, H. (2011). Identification of folding preferences of cleavage junctions of HIV-1 precursor proteins for regulation of cleavability. *J. Mol. Model.* 17, 391–399.

Okimoto, N., Futatsugi, N., Fuji, H., Suenaga, A., Morimoto, G., Yanai, R., Ohno, Y., Narumi, T., and Taiji, M. (2009). High-performance drug discovery: computational screening by combining docking and molecular dynamics simulations. *PLoS Comput. Biol.* 5:e1000528. doi: 10.1371/journal.pcbi.1000528

Onyango, C. O., Leligdowicz, A., Yokoyama, M., Sato, H., Song, H., Nakayama, E. E., Shioda, T., de Silva, T., Townend, J., Jaye, A., Whittle, H., Rowland-Jones, S., and Cotten, M. (2010). HIV-2 capsids distinguish high and low virus load patients in a West African community cohort. *Vaccine* 28(Suppl. 2), B60–B67.

Ozen, A., Haliloglu, T., and Schiffer, C. A. (2011). Dynamics of preferential substrate recognition in HIV-1 protease: redefining the substrate envelope. *J. Mol. Biol.* 410, 726–744.

Pearlman, D. A., Case, D. A., Caldwell, J. W., Ross, W. S., Cheatham, T. E. I., DeBolt, S., Ferguson, D., Seibel, G., and Kollman, P. (1995). AMBER, a package of computer programs for applying molecular mechanics, normal mode analysis, molecular dynamics and free energy calculations to simulate the structural and energetic properties of molecules. *Comp. Phys. Commun.* 91, 1–41.

Perryman, A. L., Lin, J. H., and McCammon, J. A. (2004). HIV-1 protease molecular dynamics of a wild-type and of the V82F/I84V mutant: possible contributions to drug resistance and a potential new target site for drugs. *Protein Sci.* 13, 1108–1123.

Pettit, S. C., Henderson, G. J., Schiffer, C. A., and Swanstrom, R. (2002). Replacement of the P1 amino acid of human immunodeficiency virus type 1 Gag processing sites can inhibit or enhance the rate of cleavage by the viral protease. *J. Virol.* 76, 10226–10233.

Pettit, S. C., Moody, M. D., Wehbie, R. S., Kaplan, A. H., Nantermet, P. V., Klein, C. A., and Swanstrom, R. (1994). The p2 domain of human immunodeficiency virus type 1 Gag regulates sequential proteolytic processing and is required to produce fully infectious virions. *J. Virol.* 68, 8017–8027.

Piana, S., Carloni, P., and Rothlisberger, U. (2002). Drug resistance in HIV-1 protease: flexibility-assisted mechanism of compensatory mutations. *Protein Sci.* 11, 2393–2402.

Rantalainen, K. I., Eskelin, K., Tompa, P., and Makinen, K. (2011). Structural flexibility allows the functional diversity of potyvirus genome-linked protein VPg. *J. Virol.* 85, 2449–2457.

Rantalainen, K. I., Uversky, V. N., Permi, P., Kalkkinen, N., Dunker, A. K., and Makinen, K. (2008). Potato virus A genome-linked protein VPg is an intrinsically disordered molten globule-like protein with a hydrophobic core. *Virology* 377, 280–288.

Reboul, C. F., Meyer, G. R., Porebski, B. T., Borg, N. A., and Buckle, A. M. (2012). Epitope flexibility and dynamic footprint revealed by molecular dynamics of a pMHC-TCR complex. *PLoS Comput. Biol.* 8:e1002404. doi: 10.1371/journal.pcbi.1002404

Reingewertz, T. H., Shalev, D. E., and Friedler, A. (2010). Structural disorder in the HIV-1 Vif protein and interaction-dependent gain of structure. *Protein Pept. Lett.* 17, 988–998.

Rodriguez-Barrios, F., Balzarini, J., and Gago, F. (2005). The molecular basis of resilience to the effect of the Lys103Asn mutation in non-nucleoside HIV-1 reverse transcriptase inhibitors studied by targeted molecular dynamics simulations. *J. Am. Chem. Soc.* 127, 7570–7578.

Rodriguez-Barrios, F., and Gago, F. (2004). Understanding the basis of resistance in the irksome Lys103Asn HIV-1 reverse transcriptase mutant through targeted molecular dynamics simulations. *J. Am. Chem. Soc.* 126, 15386–15387.

Sadiq, S. K., Wan, S., and Coveney, P. V. (2007). Insights into a mutation-assisted lateral drug escape mechanism from the HIV-1 protease active site. *Biochemistry* 46, 14865–14877.

Sadiq, S. K., Wright, D. W., Kenway, O. A., and Coveney, P. V. (2010). Accurate ensemble molecular dynamics binding free energy ranking of multidrug-resistant HIV-1 proteases. *J. Chem. Inf. Model.* 50, 890–905.

Sanchez, R., Pieper, U., Melo, F., Eswar, N., Marti-Renom, M. A., Madhusudhan, M. S., Mirkovic, N., and Sali, A. (2000). Protein structure modeling for structural genomics. *Nat. Struct. Biol.* 7(Suppl.), 986–990.

Sandhu, K. S. (2009). Intrinsic disorder explains diverse nuclear roles of chromatin remodeling proteins. *J. Mol. Recognit.* 22, 1–8.

Sandhu, K. S., and Dash, D. (2007). Dynamic alpha-helices: conformations that do not conform. *Proteins* 68, 109–122.

Schames, J. R., Henchman, R. H., Siegel, J. S., Sotriffer, C. A., Ni, H., and McCammon, J. A. (2004). Discovery of a novel binding trench in HIV integrase. *J. Med. Chem.* 47, 1879–1881.

Shenderovich, M. D., Kagan, R. M., Heseltine, P. N., and Ramnarayan, K. (2003). Structure-based phenotyping predicts HIV-1 protease inhibitor resistance. *Protein Sci.* 12, 1706–1718.

Shojania, S., and O'Neil, J. D. (2010). Intrinsic disorder and function of the HIV-1 Tat protein. *Protein Pept. Lett.* 17, 999–1011.

Skasko, M., Wang, Y., Tian, Y., Tokarev, A., Munguia, J., Ruiz, A., Stephens, E. B., Opella, S. J., and Guatelli, J. (2012). HIV-1 Vpu antagonizes the innate restriction factor BST-2 via lipid-embedded helix-helix interactions. *J. Biol. Chem.* 287, 58–67.

Soares, R. O., Batista, P. R., Costa, M. G., Dardenne, L. E., Pascutti, P. G., and Soares, M. A. (2010). Understanding the HIV-1 protease nelfinavir resistance mutation D30N in subtypes B and C through molecular dynamics simulations. *J. Mol. Graph. Model.* 29, 137–147.

Song, H., Nakayama, E. E., Yokoyama, M., Sato, H., Levy, J. A., and Shioda, T. (2007). A single amino acid of the human immunodeficiency virus type 2 capsid affects its replication in the presence of cynomolgus monkey and human TRIM5alphas. *J. Virol.* 81, 7280–7285.

Steven, A. C., Heymann, J. B., Cheng, N., Trus, B. L., and Conway, J. F. (2005). Virus maturation: dynamics and mechanism of a stabilizing structural transition that leads to infectivity. *Curr. Opin. Struct. Biol.* 15, 227–236.

Stoica, I., Sadiq, S. K., and Coveney, P. V. (2008). Rapid and accurate prediction of binding free energies for saquinavir-bound HIV-1 proteases. *J. Am. Chem. Soc.* 130, 2639–2648.

Takada, S. (2012). Coarse-grained molecular simulations of large

biomolecules. *Curr. Opin. Struct. Biol.* 22, 130–137.

Thorpe, I. F., and Brooks, C. L. 3rd. (2007). Molecular evolution of affinity and flexibility in the immune system. *Proc. Natl. Acad. Sci. U.S.A.* 104, 8821–8826.

Tobi, D., and Bahar, I. (2005). Structural changes involved in protein binding correlate with intrinsic motions of proteins in the unbound state. *Proc. Natl. Acad. Sci. U.S.A.* 102, 18908–18913.

Unge, T., Montelius, I., Liljas, L., and Ofverstedt, L. G. (1986). The EDTA-treated expanded satellite tobacco necrosis virus: biochemical properties and crystallization. *Virology* 152, 207–218.

van der Vries, E., Schutten, M., and Boucher, C. A. (2011). The potential for multidrug-resistant influenza. *Curr. Opin. Infect. Dis.* 24, 599–604.

Wang, J., Ma, C., Fiorin, G., Carnevale, V., Wang, T., Hu, F., Lamb, R. A., Pinto, L. H., Hong, M., Klein, M. L., and DeGrado, W. F. (2011). Molecular dynamics simulation directed rational design of inhibitors targeting drug-resistant mutants of influenza A virus M2. *J. Am. Chem. Soc.* 133, 12834–12841.

White, K. L., Chen, J. M., Margot, N. A., Wrin, T., Petropoulos, C. J., Naeger, L. K., Swaminathan, S., and Miller, M. D. (2004). Molecular mechanisms of tenofovir resistance conferred by human immunodeficiency virus type 1 reverse transcriptase containing a diserine insertion after residue 69 and multiple thymidine analog-associated mutations. *Antimicrob. Agents Chemother.* 48, 992–1003.

Wittayanarakul, K., Aruksakunwong, O., Saen-oon, S., Chantratita, W., Parasuk, V., Sompornpisut, P., and Hannongbua, S. (2005). Insights into saquinavir resistance in the G48V HIV-1 protease: quantum calculations and molecular dynamic simulations. *Biophys. J.* 88, 867–879.

Wright, D. W., and Coveney, P. V. (2011). Resolution of discordant HIV-1 protease resistance rankings using molecular dynamics simulations. *J. Chem. Inf. Model.* 51, 2636–2649.

Xu, Y., Colletier, J. P., Jiang, H., Silman, I., Sussman, J. L., and Weik, M. (2008). Induced-fit or preexisting equilibrium dynamics? lessons from protein crystallography and MD simulations on acetylcholinesterase and implications for structure-based drug design. *Protein Sci.* 17, 601–605.

Xue, B., Mizianty, M. J., Kurgan, L., and Uversky, V. N. (2012). Protein intrinsic disorder as a flexible armor and a weapon of HIV-1. *Cell. Mol. Life Sci.* 69, 1211–1259.

Yokoyama, M., Naganawa, S., Yoshimura, K., Matsushita, S., and Sato, H. (2012). Structural dynamics of HIV-1 envelope gp120 outer domain with V3 loop. *PLoS ONE* 7:e37530. doi: 10.1371/journal.pone.0037530

Yoshimoto, K., Arora, K., and Brooks, C. L. 3rd. (2010). Hexameric helicase deconstructed: interplay of conformational changes and substrate coupling. *Biophys. J.* 98, 1449–1457.

Zhou, J., Zhang, Z., Mi, Z., Wang, X., Zhang, Q., Li, X., Liang, C., and Cen, S. (2012). Characterization of the interface of the bone marrow stromal cell antigen 2-Vpu protein complex via computational chemistry. *Biochemistry* 51, 1288–1296.

Zhou, Z., Madrid, M., Evanseck, J. D., and Madura, J. D. (2005). Effect of a bound non-nucleoside RT inhibitor on the dynamics of wild-type and mutant HIV-1 reverse transcriptase. *J. Am. Chem. Soc.* 127, 17253–17260.

Conflict of Interest Statement: The authors declare that the research was conducted in the absence of any commercial or financial relationships that could be construed as a potential conflict of interest.

Received: 08 June 2012; paper pending published: 20 June 2012; accepted: 02 July 2012; published online: 19 July 2012.
Citation: Ode H, Nakashima M, Kitamura S, Sugiura W and Sato H (2012) Molecular dynamics simulation in virus research. Front. Microbio. 3:258. doi: 10.3389/fmicb.2012.00258
This article was submitted to Frontiers in Virology, a specialty of Frontiers in Microbiology.

OPEN ACCESS Freely available online

PLOS ONE

The Carboxyl-Terminus of Human Immunodeficiency Virus Type 2 Circulating Recombinant form 01_AB Capsid Protein Affects Sensitivity to Human TRIM5α

Tadashi Miyamoto[1], Emi E. Nakayama[1], Masaru Yokoyama[2], Shiro Ibe[3], Shunpei Takehara[1], Ken Kono[1], Yoshiyuki Yokomaku[3], Massimo Pizzato[4], Jeremy Luban[4], Wataru Sugiura[3], Hironori Sato[2], Tatsuo Shioda[1]*

1 Department of Viral Infections, Research Institute for Microbial Diseases, Osaka University, Suita Osaka, Japan, **2** Laboratory of Viral Genomics, Pathogen Genomics Center, National Institute of Infectious Diseases, Musashimurayama, Tokyo, Japan, **3** Department of Infection and Immunology, Clinical Research Center, National Hospital Organization Nagoya Medical Center, Naka-ku, Nagoya, Aichi, Japan, **4** Department of Microbiology and Molecular Medicine, University of Geneva, Geneva, Switzerland

Abstract

Human immunodeficiency virus (HIV) type 2 shows limited geographical distribution compared with HIV type 1. Although 8 genetic groups of HIV type 2 (HIV-2) have been described, recombinant viruses between these groups are rarely observed. Recently, three HIV-2 patients in Japan were described with rapidly progressive, acquired immunodeficiency. These patients were infected with an A/B inter-group recombinant designated CRF01_AB. Here, we characterize the capsid protein (CA) encoded by the viruses from these patients. HIV-2 CRF01_AB CA showed unique amino acid sequence almost equally distinct from group A and group B viruses. Notably, HIV-2 CRF01_AB CA showed potent resistance to human TRIM5α. In addition to the previously identified amino acid position 119 in the N-terminal domain of CA, we found that HIV-2 CRF01_AB-specific amino acid substitutions in the C-terminal domain also were necessary for resistance to human TRIM5α. These results indicate that retroviruses can evade TRIM5α by substitution at residues within the C-terminal domain of CA.

Citation: Miyamoto T, Nakayama EE, Yokoyama M, Ibe S, Takehara S, et al. (2012) The Carboxyl-Terminus of Human Immunodeficiency Virus Type 2 Circulating Recombinant form 01_AB Capsid Protein Affects Sensitivity to Human TRIM5α. PLoS ONE 7(10): e47757. doi:10.1371/journal.pone.0047757

Editor: Vladimir Brusic, Dana-Farber Cancer Institute, United States of America

Received July 31, 2012; **Accepted** September 20, 2012; **Published** October 19, 2012

Funding: This work was supported by grants from the Health Science Foundation; the Ministry of Education, Culture, Sports, Science, and Technology, Japan (23590541 to EEN, 23390111 to TS), the Ministry of Health, Labour, and Welfare, Japan (H22-AIDS-003 to HS), Swiss National Fund grant 3100A0-128655 to JL, and NIH grant RO1AI59159 to JL. The funders had no role in study design, data collection and analysis, decision to publish, or preparation of the manuscript.

Competing Interests: The authors have declared that no competing interests exist.

* E-mail: shioda@biken.osaka-u.ac.jp

Introduction

Human immunodeficiency virus type 2 (HIV-2) has been detected primarily in West Africa, in contrast to the global distribution of the type 1 epidemic virus (HIV-1). Based on molecular evidence, HIV-2 and HIV-1 are presumed to derive from simian immunodeficiency viruses that originated in sooty mangabey (SIVsm) and chimpanzee (SIVcpz), respectively, as a result of zoonotic transfer between non-human primates and human. The HIV-1 and HIV-2 bear a considerable degree of homology in both gene organization and RNA sequence (30%–60%) [1–4]. It is generally believed that HIV-2 is less pathogenic than HIV-1. However, certain HIV-2 patients with high plasma HIV-2 loads develop acquired immune deficiency syndrome (AIDS) as rapidly as HIV-1 patients do [4]. To date, eight HIV-2 groups have been distinguished on the basis of phylogenetic (sequence) analysis; each group is presumed to have originated from an independent zoonotic event [5].

TRIM5α was identified as a factor that restricts HIV-1 infection in rhesus monkey (Rh) cells [6]. TRIM5α is thought to degrade the core of the incoming virus [7,8]. TRIM5 proteins are members of the tripartite motif family containing RING, B-box, and coiled-coil domains. The alpha isoform of TRIM5 has an additional C-terminal PRYSPRY (B30.2) domain [9]. In cynomolgus monkey (CM), TRIM5α also has been demonstrated to restrict HIV-1 infection [6,10]. In contrast, the human TRIM5α exhibits minimal restriction of HIV-1 infection [11–14], but shows moderate levels of restriction for HIV-2 [15].

Capsid (CA) proteins are components of the viral core; the CAs of HIV-1 and HIV-2 have similar primary and three dimensional structures [16]. CA is composed of a surface-exposed N-terminal domain (NTD) and a C-terminal domain (CTD) that is required for oligomerization [17]. We previously identified a single amino acid of the HIV-2 capsid that determines the susceptibility of HIV-2 to CM TRIM5α. Viruses that encoded CAs with either alanine or glutamine at amino acid residue 119 (which corresponded to the 120th amino acid of the CA of the GH123 viral strain) could grow in cells harboring the CM TRIM5α. In contrast, HIV-2 encoding CA with proline at the same position showed restricted growth in cells harboring the CM TRIM5α. Similar results, although to a lesser extent, were observed when the human TRIM5α was used [15]. Furthermore, an analysis of HIV-2 CA variation in a West African Caio cohort demonstrated that the presence of proline at CA positions 119, 159, and 178 was more frequent in individuals with lower viral loads (VLs); the presence of non-proline residues at all 3 residues was more frequent in

individuals with high VLs. The *in vitro* replication levels of viruses bearing changes at the 3 positions suggested that these 3 residues influence virus replication by altering susceptibility to TRIM5α [18]. These results also suggested that TRIM5α controls virus replication in HIV-2-infected individuals.

Recently, five HIV-2-seropositive cases were identified in Japan. Three isolates (NMC307, NMC716, and NMC842) were recovered from these patients and were shown by full-length genomic analysis to represent a recombinant (designated HIV-2 CRF01_AB) of group A and B strains [19]. Although more than 75% of patients with HIV-2 have asymptomatic prognoses throughout their lifetimes [1,20], all 3 of the CRF01_AB patients were found to be at an advanced stage of AIDS with low CD4+ cell counts and high HIV-2 VLs [19]. All 3 patients were under 40 years of age when first diagnosed as HIV-2 positive [19]. Assessment of risk factors suggested that all three were infected via heterosexual contacts; no personal connection was confirmed among any of these cases [19]. In the present study, we characterized the HIV-2 CRF01_AB CA obtained from these patients and found several unique properties of HIV-2 CRF01_AB, including potent resistance to human TRIM5α-mediated restriction.

Results

HIV-2 CRF01_AB Strains Show Unique CA Sequences

Fig. 1 shows an alignment of the deduced amino acid sequences of the CAs of HIV-2 group A (ROD, UC12, GH123, and UC2), HIV-2 group B (UC14, D205, and UC1), SIVs (SIVmac239 and SIVsm PBJ14), and HIV-2 CRF01_AB (NMC307, NMC716, NMC842, and 7312A). As we reported previously [15,18], the 119th amino acid position is a proline, glutamine, or alanine in the CAs of HIV-2 group A, HIV-2 group B, and SIVs. However, the CAs of the HIV-2 CRF01_AB strains uniquely possess a glycine at this position. Based on the genomic structure of HIV-2 CRF01_AB, A/B recombinant breakpoints within this isolate are located near or within the *env* gene, such that HIV-2 CRF01_AB can be considered to consist of a group B backbone that incorporates group A *env* fragments [19]. These presumed breakpoints could be taken to suggest that CRF01_AB CA should be encoded as a B-like sequence. However, phylogenetic analysis of these CA sequences (Fig. 2) reveals that the deduced HIV-2 CRF01_AB CA proteins constitute a distinct cluster, with the dendrogram exhibiting a long branch length compared to the CAs of HIV-2 group A, HIV-2 group B, and SIV.

HIV-2 CRF01_AB CA is Highly Resistant to Human TRIM5α

In a previous study, we reported that the amino acid at residue 119 of the HIV-2 CA affects susceptibility to the restriction of virus replication by CM and human TRIM5α [15], such that HIV-2 encoding CA(Pro119) was sensitive to CM and human TRIM5α, while HIV-2 encoding CA(Gln119) or CA(Ala119) was resistant [15]. We also reported that mutation of HIV-2 strain GH123 to encode glycine at the corresponding position (GH123/G) rendered GH123 resistant to CM TRIM5α [21]. To further test the role of the CA protein in TRIM5α resistance, we generated recombinant versions of the GH123 virus (716 or 842) in which the CA-encoding segment of *gag* was replaced with that of the A/B recombinants NMC716 or NMC842 (respectively). We used a recombinant Sendai virus (SeV) system to express CM, Rh, and human TRIM5α and CM TRIM5α lacking the PRYSPRY domain as a negative control (Fig. S1). In the presence of CM TRIM5α, infection by the parental GH123 virus was restricted, but infection by GH123/G was resistant to CM TRIM5α-mediated restriction (Fig. 3A). Infection by 716 or 842 was resistant to CM TRIM5α (Fig. 3B). In contrast, infection by any of the 4 variants (GH123, GH123/G, 716, and 842) was completely restricted by Rh TRIM5α (Fig. 3A, B). These results for cells producing CM or Rh TRIM5α are consistent with our previous findings [22]. In cells producing human TRIM5α, the replication of parental GH123 and of the GH123/G mutant were partially restricted (Fig. 3A), while 716 and 842 replicated as efficiently as in negative control cells that did not produce a functional TRIM5α (Fig. 3B). The mean ratios of the p25 levels at 6 days after infection in the cells producing human TRIM5α to those in the negative control cells were 0.14 for GH123, 0.30 for GH123/G, but 0.81 for 716 and 1.02 for 842 in three independent experiments. The ratio of GH123/G was significantly higher than that of GH123 ($P = 0.0086$, t test) but lower than those of 716 ($P = 0.0059$, t test) and 842 ($P = 0.0030$, t test). Similar results were obtained when we calculated the mean ratios of the p25 levels at 3 days after infection (data not shown). These data indicate that the CA sequences of the CRF01_AB strains conferred higher potential to escape from human TRIM5α than those of GH123/G.

Viral Sensitivity to Human TRIM5α-mediated Restriction in a Single Round Infection Assay

TRIM5α restricts viral infection at a post-entry step [6,23,24]. To focus on early steps of virus replication, we performed a single-round infection assay, in which infection is detected as fluorescence generated by production of the green fluorescent protein (GFP). To construct mutant viruses encoding GFP, the fragment of GH123, 842, or GH123/G that encoded the matrix (MA) and CA proteins was transferred to the *env*-disrupted HIV-2 genomic clone pROD-env(-)-GFP, which directs the production of GFP after infection [25]. Vesicular stomatitis virus glycoprotein (VSV-G) pseudotyped wild-type and mutant HIV-2 GFP viruses were inoculated into feline CRFK cells producing TRIM5α, and GFP-positive cells were counted 2 days after infection. In this experiment, we used feline cells, since feline cells lack expression of endogenous TRIM5α. In the presence of CM TRIM5α, the numbers of GFP-positive cells were greater in cells infected with GFP-expressing viruses encoding the GH123/G or 842 CAs than in those infected with the GFP-expressing viruses encoding GH123 CA (Fig. 4), confirming that viruses encoding CA(G119) were resistant to CM TRIM5α. Consistent with the results shown in Fig. 3B, the GFP-expressing virus encoding the 842 CA from a patient was more resistant to human TRIM5α-mediated restriction than viruses encoding the CAs from GH123 ($P = 0.0010$, t-test) or GH123/G ($P = 0.0026$, t-test) (Fig. 4).

Viral Growth in TRIM5α Knock-down Cells

We next investigated whether the different resistance to human TRIM5α restriction among recombinant HIV-2 strains still applied in cells producing physiological levels of human TRIM5α protein. For this purpose, we used TRIM5α "knock-down" Jurkat cells (TRIM5α-KD Jurkat) and the corresponding control Jurkat line (Luci-siRNA Jurkat) [26]. It was demonstrated that the level of TRIM5α mRNA in TRIM5α-KD Jurkat is five times lower than that of Luci-siRNA Jurkat by TaqMan quantitative PCR. Three days after infection, GH123 replicated better in TRIM5α-KD Jurkat than in Luci-siRNA Jurkat (Fig. 5A). On the other hand, GH123/G, 716, and 842 yielded comparable titers in both cell lines (Fig. 5B, 5C, and 5D). In this experiment, we found that GH123/G also was resistant to human TRIM5α. Nevertheless, the data presented in Fig. 5 indicated that GH123 was sensitive to human TRIM5α produced at physiologically relevant levels, while 716 and 842 possessed potent resistance against human TRIM5α.

```
HIV-2A  ROD     PVQHVGG-NYTHIPLSPRTLNAWVKLVEEKKFGAEVVPGFQALSEGCTPYDINQMLNCVG  59
        UC1     ...Q.A.-....V.....................................................  59
        GH12    ...QT..G..I.V.............D.....................................  60
        UC2     ...QA..-..V.V.....................................................  59
HIV-2B  UC14    ...QIA.-..S.L.....................................................  59
        D205    ...QLA.-..V.L.....................................................  59
        UC1     ...QIA.-..V.M.....................................................  59
SIV     mac239  ...QI..-..V.L............I.....................................  59
        PBJ14   ...QI..-....L............I.....................................  59
HIV-2AB NMC307  ...Q.A.-..V.V....................I.....................................  59
        NMC716  ...Q.A.-..V.V....................I.....................................  59
        NMC842  ...Q.A.-..V.V....................I.....................................  59
        7312A   ...Q.A.-..V.V.................L.....................................  59

                                                                          119
                                                                           ↓
HIV-2A  ROD     DHQAAMQIIREIINEEAAEWDVQHPIPGPLPAGQLREPRGSDIAGTTSTVEEQIQWMFRP  119
        UC12    .................D.....................................  119
        GH123   .............D...D..A.............D..................Y..  120
        UC2     .Q..............D..A.............D.............D......Y.Q  119
HIV-2B  UC14    E................D..Q...S...M.........................Y.A  119
        D205    E................D..Q...S...M......D..................Y.A  119
        UC1     .................D..Q.............D..................Y.A  119
SIV     mac239  ..........D.......D..L...Q.A.QQ-......S.........S.D......Y.Q  118
        PBJ14   E................D..L...Q...I.P.................D......Y.Q  119
HIV-2AB NMC307  E......V..........D..Q...V..........D............P.......Y.G  119
        NMC842  E......V..........D..Q.............D.....................Y.G  119
        NMC716  E......V..........D..Q.............D.....................Y.G  119
        7312A   E......V..........D..Q...V..........D.....................Y.G  119

                                                        159       HindIII  178
                                                         ↓          ↓      ↓
HIV-2A  ROD     QNPVPVGNIYRRWIQIGLQKCVRMYNPTNILDIKQGPKEPFQSYVDRFYKSLRAEQTDPA  179
        UC12    ..............................................................  179
        GH123   ..............................V...............................  180
        UC2     ............................V..V......S................A...  179
HIV-2B  UC14    ..............L...............................................  179
        D205    ..............L...............................................  179
        UC1     ..............................................................  179
SIV     mac239  ...I..........L..............V........................A.  178
        PBJ14   ...I..........L..............V..................S........  179
HIV-2AB NMC307  ..SI..........L..............V.....................A.T.  179
        NMC716  ..S...........L..............V.....................Q.  179
        NMC842  ..S...........L..............V.....................A.T.  179
        7312A   .S.I..........L..............V.....................A.T.  179


HIV-2A  ROD     VKNWMTQTLLVQNANPDCKLVLKGLGMNPTLEEMLTACQGVGGPGQKARLM  230
        UC12    ..........I..............G.....................  230
        GH123   ..........I.....................................  231
        UC2     ..............................................  230
HIV-2B  UC14    ..........I.............................I.....  230
        D205    ..........I.............................I.....  230
        UC1     ..........I.............................I.....  230
SIV     mac239  ..........I..............V.....................  229
        PBJ14   ..........I.............I.....................  230
HIV-2AB NMC307  .RA...E................PH...........I.....  230
        NMC716  .RA...E...I............PH...........I.....  230
        NMC842  .RA...E................PH...........I.....  230
        7312A   .RA...E................PH...........I.....  230
```

Figure 1. Alignments of amino acid sequences of CA proteins encoded by selected HIV-2 isolates and SIV from the Los Alamos databases. Dots denote amino acid identity with the ROD CA; dashes denote gaps introduced to optimize alignment. HIV-2 CRF01_AB-specific amino acid residues are in red. Arrows indicate key residues at 119, 159, and 178, and the position (in the corresponding DNA sequence) of the *Hind*III restriction site used in the constructs. HIV-2A, HIV-2B, and HIV-2AB denote HIV-2 group A, HIV-2 group B, and HIV-2 CRF01_AB, respectively.
doi:10.1371/journal.pone.0047757.g001

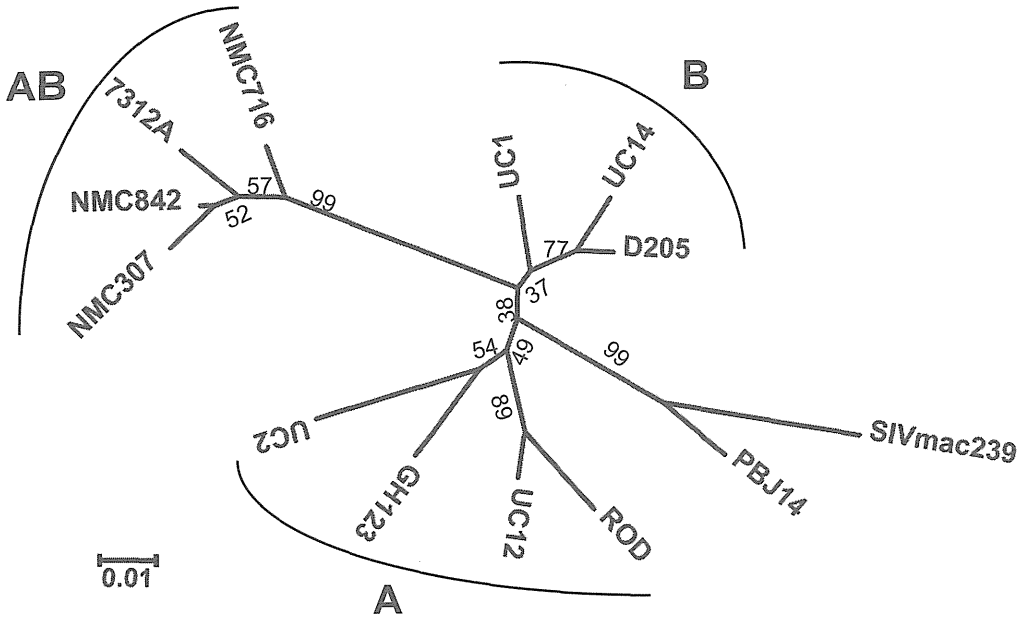

Figure 2. Phylogenetic tree of HIV-2 isolates and SIV. This phylogenetic tree was constructed by the neighbor-joining method. Bootstrap probabilities (%), as calculated by 1000 iterations, are shown at the major tree nodes. Scale bar represents 0.01 amino acid substitutions per site. A, B, and AB denote HIV-2 group A, HIV-2 group B, and HIV-2 CRF01_AB, respectively.
doi:10.1371/journal.pone.0047757.g002

Since TRIM5α-KD Jurkat always showed reduced proliferative properties compared to Luci-siRNA Jurkat (data not shown), presumably due to reduced TRIM5α levels [27], the p25 levels of all these viruses in Luci-siRNA Jurkat became higher than those in TRIM5α-KD Jurkat at 10 days after infection (data not shown).

HIV-2 CRF01_AB CA C-terminal Domain-specific Sequence also Affects Viral Sensitivity to Human TRIM5α

We previously reported that the presence of proline at CA positions 119, 159, and 178 is more frequent in individuals with lower VLs [18]. Viral isolates NMC307, NMC716, and NMC842 all encoded CAs with proline at the 159th position (Fig. 1). However, the 178th amino acid residue was encoded as a threonine (NMC307 and NMC842) or as a glutamic acid (NMC716) in these isolates (Fig. 1). To test whether a single residue at amino acid 178 of HIV-2 CRF01_AB CA affects the sensitivity to human TRIM5α, we generated recombinant 716 or 842 viruses (designated 716GPP or 842GPP, respectively) that encoded CA (Pro178) proteins. As shown in Fig. 3C, 716GPP and 842GPP escaped from human TRIM5α restriction as efficiently as 716 and 842 did. These data suggest the existence of viral determinants for human TRIM5α-resistance other than the previously identified 119th and 178th amino acid positions of CA.

To search for the viral determinants of human TRIM5α resistance other than the 119th and 178th amino acid positions of HIV-2 CA, we constructed a chimeric virus 842Hind by replacing the segment of the 842 genome that encodes CA C-terminal residues 170 to 231 with the corresponding region of GH123 (Fig. 6A). When tested in cells that produced human TRIM5α, 842 was strongly resistant to human TRIM5α as expected (Fig. 6B). However, the 842Hind construct, which encoded the NMC842 CA with the GH123 CA C-terminal short region, lost this resistance to human TRIM5α (Fig. 6C). The mean ratios of the p25 levels at 6 days after infection in the cells producing human TRIM5α to those in the negative control cells were 0.73 for 842 and 0.16 for 842Hind in three independent experiments. The ratio of 842Hind was significantly lower than that of 842 ($P = 0.0003$, t test). Similar results were obtained when we calculated the mean ratios of the p25 levels at 3 days after infection (data not shown). These results suggest that one or more of the HIV-2 CRF01_AB-specific amino acid residues within the CA C-terminal short region (Fig. 1, shown in red) also are necessary to fully evade human TRIM5α.

Molecular Dynamics of N-terminal Domain (NTD) of HIV-2 CRF01_AB CA

Residue 120 of the GH123 CA, which corresponds to residue 119 of the CRF01_AB CA, is located in the loop between α-helices 6 and 7 (L6/7) of CA NTD. Our previous molecular dynamics simulation study of HIV-2 CA NTD revealed that mutations at this position affected conformation of the neighboring loop between α-helices 4 and 5 (L4/5), and TRIM5α-sensitive viruses were predicted to share a common L4/5 conformation. In addition, the shared L4/5 structures of the sensitive viruses were associated with a decreased probability of hydrogen bond formation between GH123 CA's Asp97 (in L4/5) and Arg119 (corresponding to residue 118 in HIV-2 CRF01_AB CA; in L6/7) [21]. TRIM5α-resistant viruses exhibited a variable L4/5 conformation and a higher probability of hydrogen bond formation between L4/5 and L6/7 [21]. As noted above, HIV-2 CRF01_AB strains have a unique Gly119 (Fig. 1), which we had not previously modeled by molecular dynamics simulation. Therefore, three-dimensional (3-D) models of HIV-2 GH123/G and NMC842 CA NTD were constructed using homology modeling based on the crystal structures of the HIV-2 CA NTD, and the models were subjected to molecular dynamics simulation to compare the results with those derived from previously constructed 3-D structural models of TRIM5α-sensitive GH123 and TRIM5α-resistant GH123/Q and GH123/A [21]. GH123/Q and GH123/A encode CA (Gln120) and CA (Ala120), respectively [15]. Contrary to our expectation, the predicted L4/5 conformations of the NTDs of the NMC842 CA and GH123/G CA differed from those of

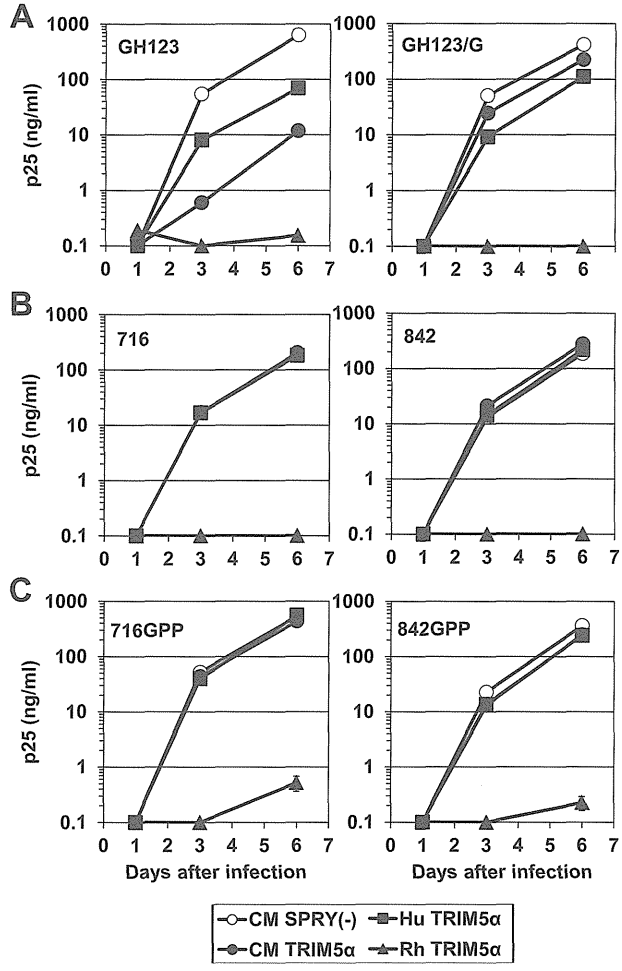

Figure 3. Growth of HIV-2 strain GH123 and variants thereof in the presence of TRIM5α. (A), (B), (C) Virus levels were measured by ELISA detection of p25 (CA) levels in supernatants. CEM-SS cells were infected with recombinant SeV encoding rhesus (Rh: black triangles); cynomolgus monkey (CM: black circles); human (Hu: black squares); or CM SPRY(-) (white circles) TRIM5α. CM SPRY (-) has a dominant negative effect on the anti-viral activity of TRIM5α and serves as a negative control. Nine hours after infection, cells were superinfected with GH123, GH123/G, 716, 842, 716GPP, or 842GPP. Error bars show actual fluctuations between levels of p25 (CA) in duplicate samples from one of three independent experiments.
doi:10.1371/journal.pone.0047757.g003

TRIM5α-resistant GH123/Q and GH123/A, better resembling that predicted for the CA NTD encoded by TRIM5α-sensitive GH123 (Fig. 7). Indeed, the calculated probability of hydrogen bond formation between L4/5 and L6/7 was even lower for the CAs of GH123/G (20.80%) and NMC842 (30.58%) compared to that of GH123 (44.6%). These results suggest that Gly119 endows the CRF01_AB CA NTD with unique structural properties.

Steric Locations of HIV-2 CRF01_AB-specific Amino Acid Substitutions

As noted above, HIV-2 CRF01_AB strains have several specific amino acid substitutions at the C-terminal domain (CTD) of CA (Fig. 1, shown in red); these substitutions were necessary for the potent resistance of these isolates against human TRIM5α (Fig. 6). Previously, we suggested that magnitudes of the computationally calculated binding energies of the CA CTD dimer models tend to be significantly greater in the TRIM5α-less-sensitive HIV-2s in

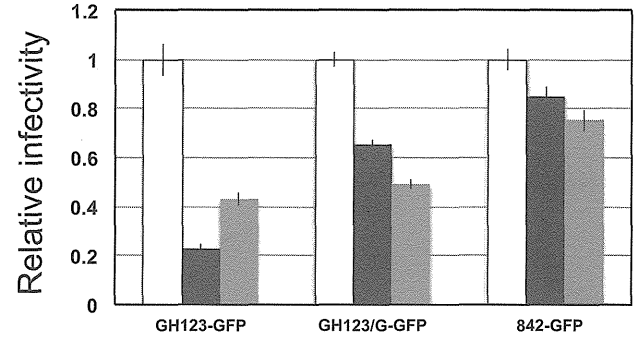

Figure 4. Viral sensitivity to TRIM5α-mediated restriction in a single-round infection assay. Feline CRFK cells were infected with SeV encoding cynomolgus monkey (CM; black bars), human (grey bars), or CM SPRY(-) (white bars) TRIM5α. CM SPRY (-) has a dominant negative effect on the anti-viral activity of TRIM5α and serves as a negative control. The cells then were superinfected with a green fluorescent protein (GFP)-expressing virus, GH123-GFP, GH123/G-GFP, or 842-GFP containing 500ng of p25 (CA). Two days after infection, the cells were fixed by formaldehyde, and GFP-producing cells were counted by flow cytometry. Numbers of GFP-positive cells in CM SPRY (-)-producing cells are set at one and relative numbers to CM SPRY (-) of GFP-positive cells are shown. Error bars denote standard deviations of triplicate samples from one of three independent experiments.
doi:10.1371/journal.pone.0047757.g004

West Africa [18]. To examine if the HIV-2 CRF01_AB-specific amino acid substitutions in CA CTD could influence the CTD-CTD dimer stability, we constructed the CA CTD dimer model of HIV-2 CRF01_AB NMC842 by homology modeling and analyzed steric locations of the specific substitutions and binding energies of the CTD dimer model. In the CA CTD dimer model of NMC842, HIV-2 CRF01_AB-specific amino acid substitutions are located in helix 9 and in the loop between helices 10 and 11, and all appeared to be situated near but distinct from the CTD-CTD dimer interface (Fig. 8A). The predicted binding energy of the CTD-CTD dimer model of the NMC842 isolate (79.6 kcal/mole) was similar to that reported in TRIM5α sensitive viruses [18]. The results may imply that the HIV-2 CRF01_AB-specific amino acid substitutions in CTD do not necessarily influence the CTD-CTD dimer stability of the TRIM5α sensitive virus.

To further obtain structural insights into the roles of these CRF01_AB-specific mutations, we analyzed their steric locations in the CA hexamer. In the hexamer model of GH123 CA that we previously constructed based on the HIV-1 CA hexamer [28], HIV-2 CRF01_AB-specific amino acid substitutions in CTD form clusters and are located at the outermost part of the hexamer (Fig. 8B and C). Notably, these substitutions exist directly under the L4/5 of neighboring CA (Fig. 8C), and most of them are clearly visible from right above (Fig. 8B). These results raise a possibility that HIV-2 CRF01_AB-specific amino acid substitutions in CA CTD may be exposed to and accessible from the outside of the viral core.

Discussion

In the present study, we have shown that the CA of HIV-2 CRF01_AB isolates have a unique feature distinct from that of other HIV-2 strains; CRF01_AB-specific sequences conferred strong resistance to human TRIM5α. In addition to the previously identified role of amino acid 119 of the CA NTD, CRF01_AB-specific amino acid substitutions in the CA CTD also were necessary for strong resistance to human TRIM5α. These amino

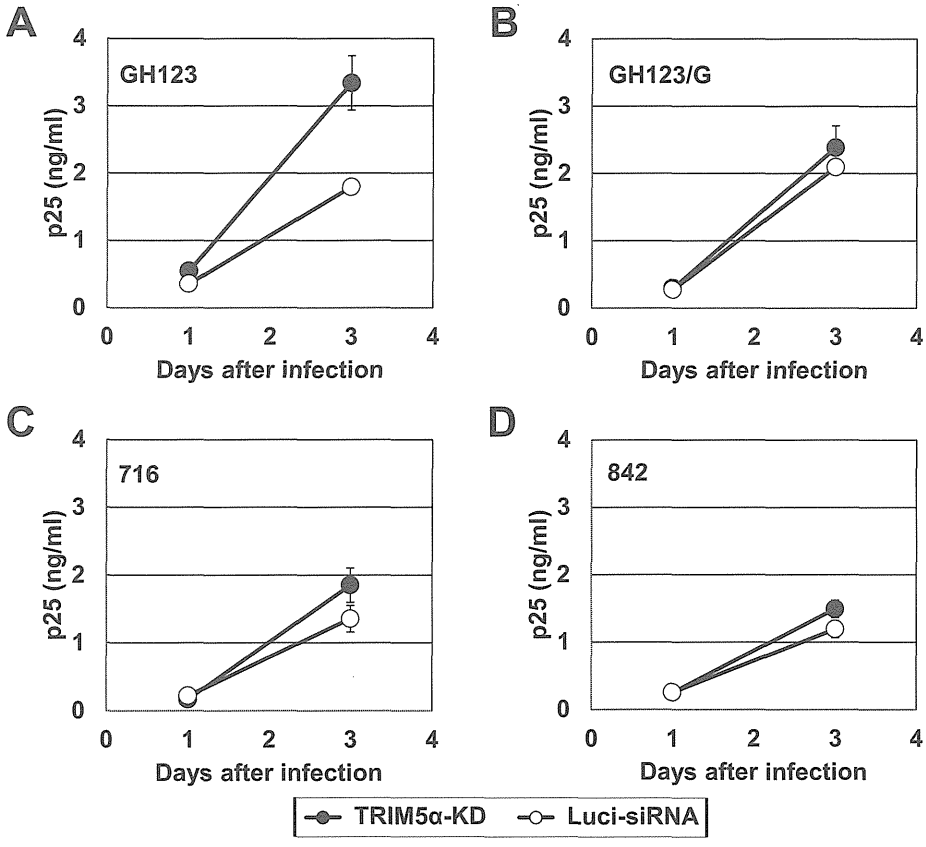

Figure 5. Viral growth in TRIM5α knock-down cells. (A), (B), (C) and (D) TRIM5α-KD Jurkat ("knock-down") or Luci-siRNA Jurkat (control) cells were infected with derivatives of GH123 virus. Culture supernatants were periodically assayed for levels of virus capsid. Error bars show actual fluctuations of duplicate samples from one of two independent experiments. Black and white bars denote TRIM5α-KD Jurkat and Luci-siRNA Jurkat cells, respectively.
doi:10.1371/journal.pone.0047757.g005

acid substitutions in CA CTD may be exposed to and accessible from the outside of the viral core.

Retroviral CA is known to form hexamers [29]. The CTD domain of retroviral capsid protein participates in CA dimerization, where intermolecular CTD-CTD interactions are mediated by symmetric, parallel dimerization of helix 9 from the CTD domains of adjacent hexamers [30]. This dimerization process is prerequisite for assemblies of multiple hexamers [29]. Previously, we found that the computationally calculated binding energies of the CA CTD dimer models could have positive relations with the TRIM5α susceptibilities of HIV-2s in West Africa [18]. We therefore calculated here the binding energy of the CTD-CTD dimer model of the NMC842 using computational method. However, the predicted binding energy of the CTD-CTD dimer of the NMC842 isolate was rather similar to that reported in TRIM5α sensitive viruses [18]. Therefore, previously undescribed mechanisms may be involved in the TRIM5α resistance of the HIV-2 CRF01_AB.

A possible mechanism for the findings may be that the CRF01_AB-specific substitutions influence directly or indirectly the structural properties of an interaction surface for the TRIM5α mediated inhibition. In this regard, we previously suggested with SIV that not only the NTD but also the CTD might constitute an intermolecular interaction surface [31]. Similarly, HIV-2 may have such interaction surface in CTD domain, and the surface may be used for the TRIM5α-mediated inhibition. Results on the steric locations of the CRF01_AB-specific substitutions in the hexamer model support this possibility (Fig. 7B and C). A preliminary modeling study of the assemblies of the CA hexamers also have supported this possibility: the NTDs are apart from each other among the hexamers, which allows to form accessible surface on the CTDs (data not shown), as suggested with Rous sarcoma virus CA [32]. Therefore, it would be interesting to examine whether HIV-2 CRF01_AB-specific amino acid substitutions in CTD could constitute a binding cleft for the TRIM5α itself or others involved in TRIM5α medicated inhibition in the assemblies of multiple CA hexamers in the viral core. Further study is necessary to address this issue.

Previously, we showed that the amino acid replacements at CA residue 119 affected the conformation of the neighboring L4/5, and that TRIM5α-sensitive viruses had a shared L4/5 conformation that was associated with a decreased probability of hydrogen bonding between L4/5 and L6/7 [21]. Although GH123/G and 842 showed resistance to TRIM5α, the calculated probability of hydrogen bond formation between L4/5 and L6/7 was lower than that calculated for the CAs of other TRIM5α-resistant viruses, including that from GH123/Q (55.15%) and GH123/A (64.47%) [21]. The conformations of L4/5 in the CAs of GH123/G and 842 also were similar to those of TRIM5α-sensitive viruses, and were distinct from those of the CAs of TRIM5α-resistant viruses. These characteristics of GH123/G and 842 were similar to those of GH123/E and GH123/D, mutant GH123 clones encoding glutamic acid and aspartic acid (respectively) at the residue corresponding to

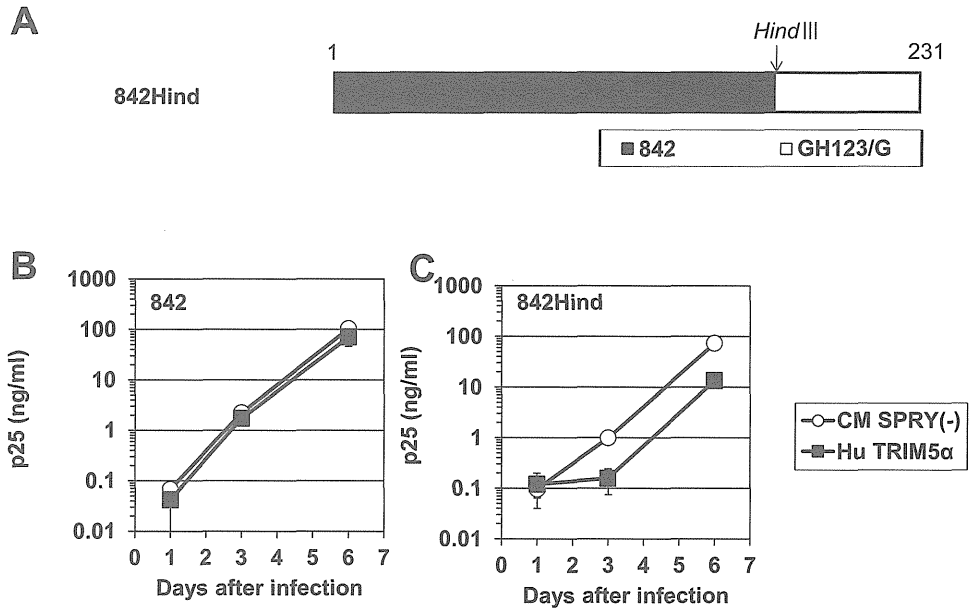

Figure 6. HIV-2 CRF01_AB CA C-terminal domain-specific sequence also affects viral sensitivity to human TRIM5α. (A) Schematic representation of chimeric viral CAs. Black and white bars show 842 and GH123/G CA peptide sequences, respectively. An arrow denotes the position (in the corresponding DNA sequence) of the *Hind*III restriction site used in the construct. (B and C) CEM-SS cells were infected with recombinant SeV encoding human (Hu: black squares) or CM SPRY(-) (white circles) TRIM5α. Nine hours after infection, cells were superinfected with 842 (B) and 842Hind (C). Culture supernatants were assayed for levels of p25 (CA). Error bars show actual fluctuations between levels of p25 (CA) in duplicate samples from one of three independent experiments.
doi:10.1371/journal.pone.0047757.g006

position 119 of HIV-2 CRF01_AB strains [21]. Although glutamic acid and aspartic acid have not been observed at this CA residue in HIV-2 isolated clinically, both GH123/E and GH123/D showed resistance against CM TRIM5α. In contrast to the CAs of GH123/Q and GH123/A, the CAs of both GH123/E and GH123/D show reduced likelihoods of hydrogen bond formation between the L4/5 and L6/7, and the L4/5 conformations were predicted to be similar to those of the CAs of TRIM5α-sensitive viruses. Therefore, our present results extend our previous observations, and additionally imply that the Gly119 of HIV-2 CRF01_AB CA prevents binding by TRIM5α, probably due to the small size of the glycine side chain. It is possible that the shared conformation of L4/5 might have some advantages in utilizing certain cellular factor(s) that bind CA. Our structural data suggests that HIV-2 CRF01_AB strains are highly adapted, since these strains have acquired potent resistance against TRIM5α without losing the shared L4/5 conformation.

In the case of GH123/E, disruption of the hydrogen bond between L4/5 and L6/7 by substitution of alanine for aspartic acid at position 97 (D97A) did not alter the resistant phenotype of GH123/E [21], while the same substitution almost completely abolished the replicative ability of GH123/G (data not shown). This result further demonstrates the unique status of GH123/G, since D97A substitution did not cause such a drastic reduction of replicative ability in GH123, GH123/Q, and GH123/A [21]. The basis for the difference between GH123/G and other variants is unclear; further mutational studies will be necessary to elucidate detailed interactions between L4/5 and L6/7, and to define the contribution of these sequences to viral replication and TRIM5α sensitivity.

In the Los Alamos databases, almost all SIV isolates encode glutamine at the position corresponding to residue 119 of the HIV-2 CRF01_AB CA. It is likely that the sequential mutation from glutamine (coded as CAA or CAG) to proline (CCA or CCG; underlines denote single nucleotide changes) and then to alanine (GCA, GCG) occurred after transmission of the monkey virus to the human population. The nature of the genetic code suggests that the Gly119-encoding virus (GGA or GGG codon) derived from the Ala119-encoding virus, implying that the viruses with glycine are highly adapted, as also discussed above. A single HIV-2 strain encoding glycine at the 119th CA residue was found in the Los Alamos databases; this strain (7312A) was isolated from a symptomatic 32-years-old man [33], and also was a recombinant between groups A and B (Fig. 1 and 2). This recombinant virus exhibits a genomic organization similar to that of NMC307, NMC716, and NMC842. At present, we do not know whether the emergence of glycine at the 119th position of CA is unique to HIV-2 CRF01_AB. It will be critical to assess the emergence of Gly119 viruses within HIV-2 groups A and B.

It is generally believed that HIV-2 is less pathogenic than HIV-1, and the number of HIV-2 cases is now gradually decreasing in West Africa. However, NMC307, NMC716, and NMC842 were recovered from patients at an advanced stage of AIDS with low CD4+ cell counts and high HIV-2 VLs [19]. It is possible that these HIV-2 CRF01_AB strains are highly pathogenic, unlike other HIV-2 strains. Careful epidemiological and virological studies are necessary to test this hypothesis. In the present study, we found that HIV-2 CRF01_AB CA confers strong resistance to human TRIM5α. In the Caio HIV-2 cohort in West Africa, non-proline residues at position 119 were significantly associated with elevated plasma HIV-2 load [18]. Therefore, resistance to TRIM5α may at least partially explain why these 3 patients in Japan developed AIDS so rapidly, although the possible effects of mutations in regions (e.g., *env*, *vif*, *nef* and the long terminal repeats) other than those that encode CA cannot be fully excluded at

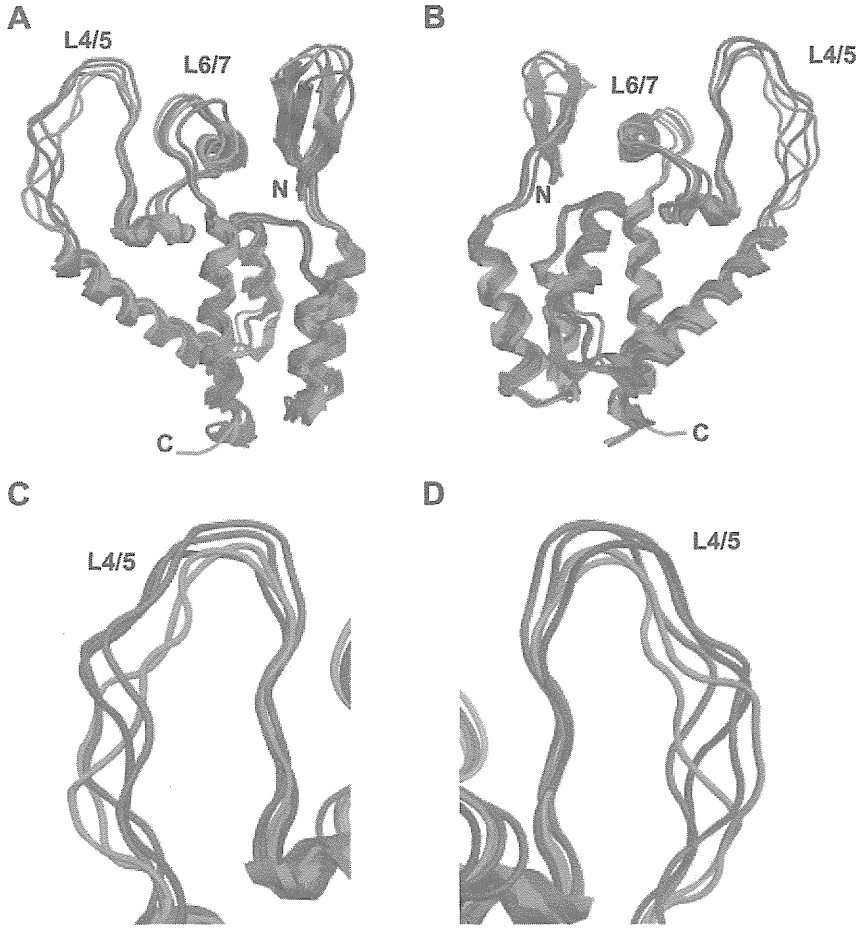

Figure 7. Structural models of the HIV-2 capsid N-terminal domain. Models were constructed by homology modeling and molecular dynamics simulations with the high-resolution X-ray crystal structure of the HIV-2 capsid N-terminal domain (CA NTD) (PDB code: 2WLV [16]) as the starting structure. Averaged conformations of the overall structure of the CA NTD (from the amino acid position 1 to 150) during 5–20 nanoseconds of MD simulations (A and B) and a close-up view around the L4/5 loop (C and D) are indicated. N and C indicate the amino termini and carboxyl termini, respectively. Models are color coded as follows: red, 842; blue, GH123/G; green, CM TRIM5α-resistant viruses (GH123/Q and GH123/A); and purple, CM TRIM5α-sensitive virus (GH123/P).
doi:10.1371/journal.pone.0047757.g007

present. Our results also suggest that resistance to TRIM5α might be a new marker for the pathogenic potential of HIV-2. The possible emergence of a highly pathogenic HIV-2 strain is an ongoing concern, given that retroviruses can easily evolve to evade host defenses.

Materials and Methods

Phylogenetic Tree Analysis

Multiple sequence alignment was performed using the software CLUSTALW version 2.1. Phylogenetic trees were constructed using the neighbor-joining method. Bootstrap probabilities were calculated by 1000 iterations [34].

Cell Culture

The human 293T [35] and feline CRFK [36] cells were maintained in Dulbecco's Modified Eagle medium. The human T-cell line CEM-SS [37] was maintained in RPMI medium. All media were supplemented with 10% fetal bovine serum and 1% penicillin-streptomycin.

Plasmid Construction

Recombinant HIV-2 GH123 clones containing the entire CA sequence of the isolates NMC716 or NMC842 (716 or 842, respectively) and 716 or 842 with proline substitutions at the 178th position (716GPP or 842GPP, respectively) were generated by PCR-based mutagenesis. The GH123/G virus was described previously [21]. The 0.6-kb *Hind*III-*Xho*I fragment of 842 was replaced with the corresponding fragment of GH123/G, and the resulting plasmid was designated 842Hind. Infectious viruses were prepared by transfection of 293T cells with the resulting proviral DNA clones. Viral titers were determined by measuring P25 (CA) with a RetroTek antigen ELISA kit (ZeptoMetrix, Buffalo, NY).

To construct the wild-type and mutant HIV-2 clones encoding GFP, the 1.6-kb *Kpn*I-*Xho*I fragment (which encodes the MA, CA and p6) of GH123, 842, or GH123/G, was transferred to pROD-env(-)-GFP [25], a clone in which the *env* gene is disrupted, and the GFP gene was inserted into the *nef* region. Infectious viruses were prepared by transfection of 293T cells with proviral DNA clones together with the pMD2G plasmid encoding VSV-G. Viral titers were determined as above.

Construction of recombinant SeV encoding C-terminally HA-tagged CM TRIM5α (CM-TRIM5α-SeV), Rh TRIM5α (Rh-

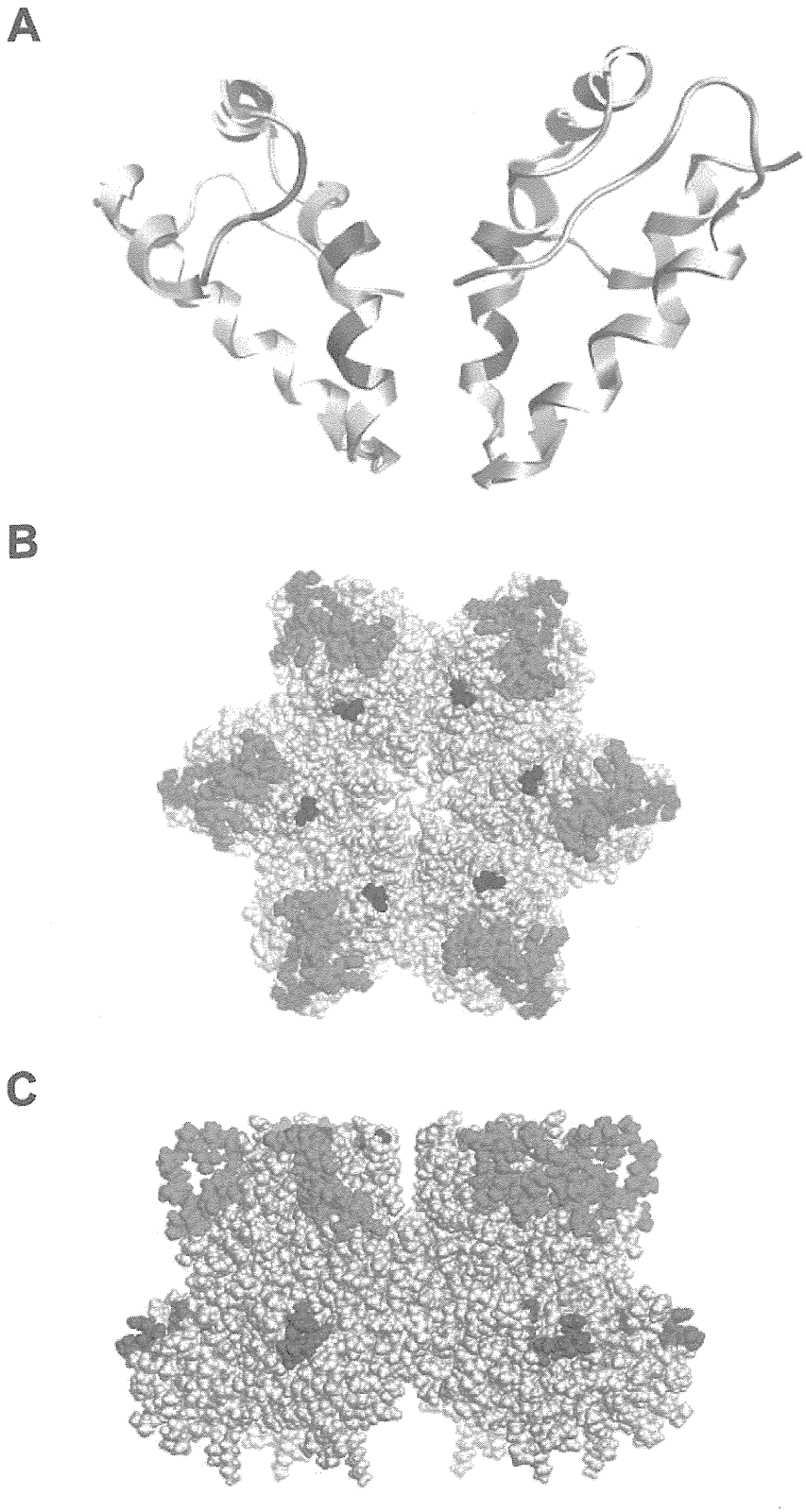

Figure 8. Structural models of the HIV-2 capsid C-terminal domain in dimeric form (A) and the HIV-2 GH123 capsid hexamer (B and C). (A) The C-terminal domain dimer model (from the amino acid position 150 to 219) of HIV-2 capsid (CA) is based on the viral sequence of NMC842. HIV-2 CRF01_AB-specific amino acid substitutions are shown in red. (B and C) The space-filling model of CA hexamer from the top (B) and side (C) is shown. Positions of HIV-2 CRF01_AB-specific amino acid substitutions are shown in red. L4/5 and 120P are shown in green and blue, respectively.
doi:10.1371/journal.pone.0047757.g008

TRIM5α-SeV), human TRIM5α (Hu-TRIM5α-SeV), and CM TRIM5α lacking the PRYSPRY domain (CM-SPRY(-)-SeV) were described previously [10,15,22].

Viral Infection

CEM-SS cells (1×10^6) were infected with SeVs encoding the respective TRIM5α proteins at a multiplicity of infection of 10 plaque-forming units per cell and incubated at 37°C for 9 h. Aliquots of 1×10^5 cells were then superinfected with GH123, GH123/G, 716, 716GPP, 842, 842GPP, or 842Hind virus. Each superinfection used a titer of virus corresponding to 20 ng of p25 (CA). Experiment was performed three separate times with duplicate samples. For viral infection of cells producing physiological levels of TRIM5α, TRIM5α knock-down Jurkat cells (TRIM5α-KD Jurkat) and control cells (Luci-siRNA Jurkat) were infected with GH123, GH123/G, 716, or 842 virus. Each infection used a titer of virus corresponding to 100 ng of p25. The culture supernatants were collected periodically, and the level of p25 (CA) was measured as described above. Experiment was performed two separate times with duplicate samples.

Western Blot

CEM-SS cells (1×10^6) infected with recombinant SeVs expressing HA-tagged TRIM5α proteins were lysed in lysis buffer (50 mM Tris-HCl, pH 7.5, 150 mM NaCl, 1% Nonidet P40, 0.5% sodium deoxycholate). TRIM5α proteins in the lysates were subjected to sodium dodecyl sulfate-polyacrylamide gel electrophoresis. Proteins in the gel were then electronically transferred onto a membrane (Immobilon; Millipore, Billerica, MA). Blots were blocked and probed with anti-HA high-affinity rat monoclonal antibody (Roche, Indianapolis, IN) overnight at 4°C. Blots were then incubated with peroxidase-conjugated anti-rat IgG (American Qualex, San Clemente, CA), and bound antibodies were visualized with a Chemilumi-One chemiluminescent kit (Nacalai Tesque, Kyoto, Japan).

Single-round Infection Assay

SeV-infected CRFK cells (4×10^4) were infected with a titer of pROD-env(-)-GFP derivative virus corresponding to 500 ng of p25 (CA). Two days after infection, the cells were fixed by formaldehyde, and GFP-producing cells were counted by flow cytometry. Experiment was performed three separate times with triplicate samples.

Molecular Modeling and MD Simulation

We used molecular dynamic (MD) simulations [38] to analyze the structural dynamics of the HIV-2 CA NTDs. First, initial CA structures for MD simulation were constructed by homology modeling [39] using the Molecular Operating Environment, MOE (Chemical Computing Group Inc., Montreal, Canada) as described previously [15,40]. We used the high-resolution crystal structure of the HIV-2 CA NTD at a resolution of 1.25Å (PDB code: 2WLV) [16] as the modeling template. Structural dynamics of these HIV-2 CA models in an aqueous environment were analyzed using MD simulations with the SANDER module in the AMBER 9 program package [41] and the AMBER99SB force field with the TIP3P water model [42]. Bond lengths involving hydrogen were constrained with SHAKE [43] and the time step for all MD simulations was set to 2 fs. After heating calculations for 20 ps to 310 K using the NVT ensemble, the simulations were executed using the NPT ensemble at 1 atm and 310 K for 20 ns. Hydration analyses were performed using the ptraj module in AMBER. A maximum cut-off angle of 120.0° and cut-off length of 3.5 Å were used in hydrogen bond definitions.

For the CTD dimer model of HIV-2 CRF01_AB NMC842, a crystal structure of the HIV-1 CA protein was used as the template for the modeling; the dimer of CA C-terminal domain at a resolution of 1.70 Å (PDB code: 1A8O) [17]. The amino acid sequence identity of HIV-1 (1A8O) and HIV-2 CA (NMC842 in this study) is about 76%. The sequence similarity is sufficient to construct a structural model with an r.m.s. deviation of approximately 1.5 Å for the main chain between the predicted and actual structures [39]. The 3-D structures were optimized thermodynamically by energy minimization using MOE and an AMBER99 force field [44] and further refined the physically unacceptable local structures on the basis of evaluation of unusual dihedral angles, *phi* and *psi*, by the Ramachandran plot using MOE. The binding energies of the CA dimer models, E_{bind}, were calculated as described elsewhere [45,46], using the formula $E_{bind} = E_{dimer} - 2E_{monomer}$, where E_{dimer} is the energy of the CA dimer; $E_{monomer}$ is the energy of the CA monomer.

Conclusions

The CA of HIV-2 CRF01_AB isolates have a unique feature distinct from that of other HIV-2 strains; CRF01_AB-specific sequences conferred strong resistance to human TRIM5α. CRF01_AB-specific amino acid substitutions in the CA CTD were necessary for strong resistance to human TRIM5α.

Supporting Information

Figure S1 Western blot analysis of TRIM5α proteins. HA-tagged TRIM5α proteins in lysate of CEM-SS cells infected with recombinant SeV were visualized by western blotting with an antibody against HA. S(-), Hu, CM, and Rh denote CM SPRY(-), human, cynomolgus monkey, and rhesus TRIM5α, respectively. Molecular weight makers are shown on the left.
(EPS)

Acknowledgments

We thank Dr. Y. Tian, Dr. S. Nakamura and Dr. T. Yasunaga for helpful discussions, and Ms. S. Bando and Ms. N. Teramoto for assistance.

Author Contributions

Conceived and designed the experiments: TM EEN SI HS TS. Performed the experiments: TM EEN MY ST KK. Analyzed the data: TM EEN MY SI KK JL WS HS TS. Contributed reagents/materials/analysis tools: SI YY MP JL WS. Wrote the paper: TM EEN MY SI JL HS TS.

References

1. Rowland-Jones SL, Whittle HC (2007) Out of Africa: what can we learn from HIV-2 about protective immunity to HIV-1? Nat Immunol 8: 329–331.
2. Gao F, Bailes E, Robertson DL, Chen Y, Rodenburg CM, et al. (1999) Origin of HIV-1 in the chimpanzee Pan troglodytes troglodytes. Nature 397: 436–441.
3. Huet T, Cheynier R, Meyerhans A, Roelants G, Wain-Hobson S (1990) Genetic organization of a chimpanzee lentivirus related to HIV-1. Nature 345: 356–359.
4. Gottlieb GS, Sow PS, Hawes SE, Ndoye I, Redman M, et al. (2002) Equal plasma viral loads predict a similar rate of CD4+ T cell decline in human immunodeficiency virus (HIV) type 1- and HIV-2-infected individuals from Senegal, West Africa. J Infect Dis 185: 905–914.
5. Damond F, Worobey M, Campa P, Farfara I, Colin G, et al. (2004) Identification of a highly divergent HIV type 2 and proposal for a change in HIV type 2 classification. AIDS Res Hum Retroviruses 20: 666–672.
6. Stremlau M, Owens CM, Perron MJ, Kiessling M, Autissier P, et al. (2004) The cytoplasmic body component TRIM5alpha restricts HIV-1 infection in Old World monkeys. Nature 427: 848–853.

7. Sebastian S, Luban J (2005) TRIM5alpha selectively binds a restriction-sensitive retroviral capsid. Retrovirology 2: 40.
8. Stremlau M, Perron M, Lee M, Li Y, Song B, et al. (2006) Specific recognition and accelerated uncoating of retroviral capsids by the TRIM5alpha restriction factor. Proceedings of the National Academy of Sciences of the United States of America 103: 5514–5519.
9. Reymond A, Meroni G, Fantozzi A, Merla G, Cairo S, et al. (2001) The tripartite motif family identifies cell compartments. Embo J 20: 2140–2151.
10. Nakayama EE, Miyoshi H, Nagai Y, Shioda T (2005) A specific region of 37 amino acid residues in the SPRY (B30.2) domain of African green monkey TRIM5alpha determines species-specific restriction of simian immunodeficiency virus SIVmac infection. Journal of Virology 79: 8870–8877.
11. Hatziioannou T, Perez-Caballero D, Yang A, Cowan S, Bieniasz PD (2004) Retrovirus resistance factors Refl and Lv1 are species-specific variants of TRIM5alpha. Proceedings of the National Academy of Sciences of the United States of America 101: 10774–10779.
12. Keckesova Z, Ylinen LM, Towers GJ (2004) The human and African green monkey TRIM5alpha genes encode Refl and Lv1 retroviral restriction factor activities. Proceedings of the National Academy of Sciences of the United States of America 101: 10780–10785.
13. Perron MJ, Stremlau M, Song B, Ulm W, Mulligan RC, et al. (2004) TRIM5alpha mediates the postentry block to N-tropic murine leukemia viruses in human cells. Proceedings of the National Academy of Sciences of the United States of America 101: 11827–11832.
14. Nakayama EE, Shioda T (2010) Anti-retroviral activity of TRIM5 alpha. Rev Med Virol 20: 77–92.
15. Song H, Nakayama EE, Yokoyama M, Sato H, Levy JA, et al. (2007) A single amino acid of the human immunodeficiency virus type 2 capsid affects its replication in the presence of cynomolgus monkey and human TRIM5alphas. Journal of Virology 81: 7280–7285.
16. Price AJ, Marzetta F, Lammers M, Ylinen LM, Schaller T, et al. (2009) Active site remodeling switches HIV specificity of antiretroviral TRIMCyp. Nat Struct Mol Biol 16: 1036–1042.
17. Gamble TR, Yoo S, Vajdos FF, von Schwedler UK, Worthylake DK, et al. (1997) Structure of the carboxyl-terminal dimerization domain of the HIV-1 capsid protein. Science 278: 849–853.
18. Onyango CO, Leligdowicz A, Yokoyama M, Sato H, Song H, et al. (2010) HIV-2 capsids distinguish high and low virus load patients in a West African community cohort. Vaccine 28S2: B60–B67.
19. Ibe S, Yokomaku Y, Shiino T, Tanaka R, Hattori J, et al. (2010) HIV-2 CRF01_AB: first circulating recombinant form of HIV-2. J Acquir Immune Defic Syndr 54: 241–247.
20. Marlink R, Kanki P, Thior I, Travers K, Eisen G, et al. (1994) Reduced rate of disease development after HIV-2 infection as compared to HIV-1. Science 265: 1587–1590.
21. Miyamoto T, Yokoyama M, Kono K, Shioda T, Sato H, et al. (2011) A single amino acid of human immunodeficiency virus type 2 capsid protein affects conformation of two external loops and viral sensitivity to TRIM5alpha. PloS one 6: e22779.
22. Kono K, Song H, Shingai Y, Shioda T, Nakayama EE (2008) Comparison of anti-viral activity of rhesus monkey and cynomolgus monkey TRIM5alphas against human immunodeficiency virus type 2 infection. Virology 373: 447–456.
23. Wu X, Anderson JL, Campbell EM, Joseph AM, Hope TJ (2006) Proteasome inhibitors uncouple rhesus TRIM5alpha restriction of HIV-1 reverse transcription and infection. Proceedings of the National Academy of Sciences of the United States of America 103: 7465–7470.
24. Anderson JL, Campbell EM, Wu X, Vandegraaff N, Engelman A, et al. (2006) Proteasome inhibition reveals that a functional preintegration complex intermediate can be generated during restriction by diverse TRIM5 proteins. Journal of Virology 80: 9754–9760.
25. Pertel T, Reinhard C, Luban J (2011) Vpx rescues HIV-1 transduction of dendritic cells from the antiviral state established by type 1 interferon. Retrovirology 8: 49.
26. Sokolskaja E, Berthoux L, Luban J (2006) Cyclophilin A and TRIM5alpha independently regulate human immunodeficiency virus type 1 infectivity in human cells. Journal of Virology 80: 2855–2862.
27. Pertel T, Hausmann S, Morger D, Zuger S, Guerra J, et al. (2011) TRIM5 is an innate immune sensor for the retrovirus capsid lattice. Nature 472: 361–365.
28. Kono K, Song H, Yokoyama M, Sato H, Shioda T, et al. (2010) Multiple sites in the N-terminal half of simian immunodeficiency virus capsid protein contribute to evasion from rhesus monkey TRIM5alpha-mediated restriction. Retrovirology 7: 72.
29. Pornillos O, Ganser-Pornillos BK, Kelly BN, Hua Y, Whitby FG, et al. (2009) X-ray structures of the hexameric building block of the HIV capsid. Cell 137: 1282–1292.
30. Ganser-Pornillos BK, Yeager M, Sundquist WI (2008) The structural biology of HIV assembly. Curr Opin Struct Biol 18: 203–217.
31. Inagaki N, Takeuchi H, Yokoyama M, Sato H, Ryo A, et al. (2010) A structural constraint for functional interaction between N-terminal and C-terminal domains in simian immunodeficiency virus capsid proteins. Retrovirology 7: 90.
32. Bailey GD, Hyun JK, Mitra AK, Kingston RL (2012) A structural model for the generation of continuous curvature on the surface of a retroviral capsid. J Mol Biol 417: 212–223.
33. Gao F, Yue L, White AT, Pappas PG, Barchue J, et al. (1992) Human infection by genetically diverse SIVSM-related HIV-2 in west Africa. Nature 358: 495–499.
34. Hillis DM, Bull JJ (1993) An empirical test of bootstrapping as a method for assessing confidence in phylogenetic analysis. Syst Biol 42: 182–192.
35. Pear WS, Nolan GP, Scott ML, Baltimore D (1993) Production of high-titer helper-free retroviruses by transient transfection. Proc Natl Acad Sci U S A 90: 8392–8396.
36. Lasfargues EY, Lasfargues JC, Dion AS, Greene AE, Moore DH (1976) Experimental infection of a cat kidney cell line with the mouse mammary tumor virus. Cancer Res 36: 67–72.
37. Sheehy AM, Gaddis NC, Choi JD, Malim MH (2002) Isolation of a human gene that inhibits HIV-1 infection and is suppressed by the viral Vif protein. Nature 418: 646–650.
38. Dodson GG, Lane DP, Verma CS (2008) Molecular simulations of protein dynamics: new windows on mechanisms in biology. EMBO Rep 9: 144–150.
39. Baker D, Sali A (2001) Protein structure prediction and structural genomics. Science 294: 93–96.
40. Shirakawa K, Takaori-Kondo A, Yokoyama M, Izumi T, Matsui M, et al. (2008) Phosphorylation of APOBEC3G by protein kinase A regulates its interaction with HIV-1 Vif. Nat Struct Mol Biol 15: 1184–1191.
41. Case DA, Darden TA, Cheatham I, T.E., Simmerling CL, Wang JR, et al. (2006) AMBER 9. University of California, San Francisco.
42. Hornak V, Abel R, Okur A, Strockbine B, Roitberg A, et al. (2006) Comparison of multiple Amber force fields and development of improved protein backbone parameters. Proteins 65: 712–725.
43. Ryckaert J-P, Ciccotti G, Berendsen HJC (1977) Numerical integration of the cartesian equations of motion of a system with constraints: Molecular dynamics of n-alkanes. J Comput Phys 23: 327–341.
44. Ponder JW, Case DA (2003) Force fields for protein simulations. Adv Protein Chem 66: 27–85.
45. Lee K, Chu CK (2001) Molecular modeling approach to understanding the mode of action of L-nucleosides as antiviral agents. Antimicrob Agents Chemother 45: 138–144.
46. Kinomoto M, Yokoyama M, Sato H, Kojima A, Kurata T, et al. (2005) Amino acid 36 in the human immunodeficiency virus type 1 gp41 ectodomain controls fusogenic activity: implications for the molecular mechanism of viral escape from a fusion inhibitor. Journal of Virology 79: 5996–6004.